Internal flow variations and diachronous sedimentation within extensive, sustained, density-stratified pyroclastic density currents flowing down gentle slopes, as revealed by the internal architectures of well-exposed ignimbrites on Tenerife

Richard J. Brown[1] and Michael J. Branney[2]

[1]Department of Earth Sciences, Durham University, Durham, DH1 3LE, UK

[2]Geology Department, University of Leicester, University Road, Leicester, LE1 7RH, UK

*Corresponding author: richard.brown3@durham.ac.uk

ABSTRACT

During a protracted explosive eruption, at least four laterally extensive and sustained pyroclastic density currents radiated across the flanks of Las Cañadas volcano, Tenerife. Each pyroclastic current developed marked local and regional spatial variations in response to the incised, gently concave substrate topography. The locations of these variations shifted in space as rapid sedimentation from the current progressively buried and modified the topography. This complex, shifting response of the density currents to minor topographic variations has been reconstructed in high-resolution over a wide area (>500 km^2) using the internal architecture of cryptic time-surfaces ('entrachrons') marked by compositional zoning in the deposit, including variations in clast types. Valley-side field relations reveal that the currents were density-stratified. At a single instant in time, the lower levels of each current comprised a granular-fluid at some locations but were fully dilute and turbulent at others. However, the locations of these variations shifted geographically as the topography changed during the eruption. The variations within the current are recorded by numerous superbly-exposed gradational transitions from various stratified to massive lithofacies, both laterally and in the downcurrent

direction. Individual currents were regionally widespread and travelled >15 km, but deposited only in longitudinally-restricted, localised zones that spanned several small valleys and interfluves. The currents bypassed slopes upcurrent and downcurrent of the restricted depositional zones, without depositing. The locations of deposition then gradually shifted with time, such that the extensive deposit sheet was gradually assembled beneath the sustained current in a diachronous fashion. Onlap relationships of internal entrachrons reveal that the base of the ignimbrite sheet and even the bases of individual flow-units are markedly diachronous. Deposition of a flow-unit commenced and ceased at different times in different places. This study suggests that in hazard assessments: (A) models of density currents that incorporate only pre-existing topography (e.g. from DEMs) may give misleading results in the case od sustained currents, because sedimentation from these significantly modifies the topography during emplacement, altering flow paths; (B), frequencies and scales of previous pyroclastic currents determined from pyroclastic successions are likely to be significantly under-estimated because currents commonly bypass without leaving a deposit record; and (C) even where preservation appears to be complete, an ignimbrite at a single exposure commonly will not record the current's entire flow history at that site.

Keywords: ignimbrite, pyroclastic density current, topography, volcanic hazard, Plinian eruption

Introduction

How density currents interact with substrate topography is of interest to workers on marine turbidite basins, volcanoes, and flood-prone regions (e.g., Fisher 1990, 1995; Valentine et al. 1992; Alexander and Morris 1994; De Rita et al. 1998; Kneller and McCaffrey 1999; Bursik and Woods 2000; Legros and Kelfoun 2000; Kubo 2004; Sulpizio et al. 2008; Doronzo et al. 2010; Gurioli et al. 2010; Lube et al. 2011; Andrews and Manga 2011; Doronzo and Dellino 2012). It is of particular importance to those who work on volcanic hazards at densely populated volcanoes (e.g., Bourdier and Abdurachman 2001; Lirer et al. 2001; Rossano et al. 2004; see also Doronzo and Dellino 2012; Gertisser et al., 2012).

Deposition from particulate gravity currents is fundamentally influenced by substrate topography, and most volcanoes are characterised by substantial relief (e.g., cones, craters and calderas) and many are incised by gullies and valleys. Deposition from density currents typically relates to decelerations resulting from flow divergence (radial flow) or flow down concave slopes (depletive flow; Kneller and Branney 1995; Branney and Kokelaar 2002), including across breaks-in-slope at the base of a volcanic cone, or as a result of encounters with an obstacle in the flow path, as demonstrated in the field, in the laboratory and through modelling (e.g., Valentine, 1987; Macias et al. 1998; Woods et al. 1998; Sulpizio et al. 2007, 2008, 2010; Gurioli et al., 2010; see reviews by Druitt 1998; Branney and Kokelaar 2002; Sulpizio and Dellino 2008). In the past decade, understanding the nature and behaviour of pyroclastic density currents (PDCs) has gained from focus on observed small-volume dome-collapse and Vulcanian eruptions (e.g., Calder et al. 1999; Loughlin et al. 2002; Druitt et al. 2002). Witnessed currents of this type were small-volume, short-lived and depletive, and affected relatively small areas, mostly along valley floors. In contrast, large-volume, radiating PDCs, associated with some large Plinian eruptions, pose a far greater hazard: they are regionally extensive, and they inundate vast areas including over topographic highs within just seconds to hours.

This paper focuses on large-volume radiating density currents, to explore (A) the role of topography, of a range of scales, in influencing deposition from a density current, and (B) how topography changes as a result of deposition by the current. Our analysis draws on an extensive data set of a complex, 3-dimensional internal architecture within a low-aspect ratio ignimbrite sheet, the 273 ka Poris ignimbrite on Tenerife (Edgar et al 2002; Brown et al 2003; Brown and Branney 2004a). This deposit is widespread and was deposited by at least four sustained pyroclastic density currents across irregular topography (Brown and Branney 2004a). The Poris ignimbrite is instructive because it is laterally widespread (500 km^3), compositionally zoned and particularly well-exposed and dissected: these features are not commonly presented together. Detailed logging of 85 vertical sections has enabled us to trace time-surfaces (‘entrachrons’ of Branney and Kokelaar 2002) through the interior of the ignimbrite sheet from valley-to-valley across interfluves and ridges, and also in the downcurrent

direction. This has allowed us to reconstruct temporal and spatial variations within the sustained currents on both local and regional scales; how these variations evolved rapidly during the eruption; and how deposition from each density current was highly localised and accompanied by widespread bypassing, resulting in a patchy, incomplete record of the flow history at any individual location. We regard such density current behaviour to typify the behaviour of larger, prolonged density currents on gentle slopes, this increases the potential to underestimate the frequency, duration and dispersal of PDCs in field studies. The study illustrates the importance of meticulous fieldwork in determining the hazards posed by PDC-forming eruptions at large volcanoes. This is of particular importance for volcanoes near the sea because much of the depositional mass transported by PDCs may end-up concealed offshore**.**

The sedimentation of ignimbrite

The depositional mechanisms of catastrophic currents that produce large ignimbrites are thought to be gradational between fluid-modified granular flows and particle-bearing fluids (Branney and Kokelaar 2002). Such gradational currents are poorly understood. Direct observation of their deposition is impossible, not least because they are capricious, opaque and hazardous. Over the past three decades studies on the architecture of large ignimbrite sheets (e.g., Taupo ignimbrite, New Zealand, Wilson and Walker 1985; Valley of Ten Thousand Smokes ignimbrite, Alaska, Fierstein and Hildreth 1992; Fierstein and Wilson 2005; 1991 eruption of Pinatubo, Philippines, Scott et al. 1996; Branney and Kokelaar 2002; Zaragoza ignimbrite, Mexico, Carrasco-Nüñez and Branney 2005) have provided insights into the depositional mechanisms of PDCs. Our understanding of the transport and deposition of ignimbrite derives largely from inferences from such deposits, from laboratory experiments (e.g. Choux and Druitt, 2002; Roche et al. 2005, 2011; Girolami et al. 2010; Roche 2012) and the numerical modelling of selected physical parameters (e.g. Valentine 1987; Dade and Huppert 1996; Woods et al 1998; Druitt 1998; Denlinger and Iverson 2001; Burgisser and Bergantz 2002; Dufek et al., 2009; Doronzo et al. 2010; Andrews and Manga 2012). However, models and experiments are not yet

sufficiently sophisticated to account for the range of common ignimbrite lithofacies, nor their complex architectures.

Large-volume ignimbrites derive from protracted currents that may last for minutes to hours (e.g., 1991 eruption of Pinatubo, Philippines, Scott et al. 1996). The deposits of sustained particulate density currents can be complex, and exhibit rapid vertical and lateral lithofacies transitions (e.g. Scott et al. 1996; Bryan et al. 1998b; Allen and Cas 1998; Brown and Branney 2004a, 2004b; Pittari et al. 2006). This complexity has led workers to consider that sustained currents are inhomogeneous in both space and time, i.e., their velocity, concentration, capacity and rheology can change spatially and temporally during transport and deposition (e.g., Branney and Kokelaar 1992, 2002; Kneller and McCaffrey 1991; Best et al. 2005; Andrews and Manga 2012). In such currents a range of different clast-support mechanisms operate in tandem during transport and deposition (Branney and Kokelaar 2002), so that adjacent clasts within the resulting ignimbrite may have had different transport histories. Flow directions of sustained density currents also vary with time at individual locations (Kneller et al. 1999; Morris and Alexander 2003; Branney et al. 2004; Andrews and Branney 2012).

The depositional mechanisms of sustained PDCs are fundamentally influenced by lower flow-boundary conditions, which as the result of density stratification in the current will differ significantly from conditions higher in the current (Fisher 1966; Valentine 1987; Branney and Kokelaar 1992, 1997, 2002; Sohn 1997; Sulpizio et al. 2007; Sulpizio and Dellino, 2008). The flow-boundary zone includes the basal part of the current and the uppermost part of the deposit, and it rises as the deposit aggrades. Over the past decade researchers have recognised a continuum of flow-boundary zone conditions that give rise to a range of PDC deposit types as a function of current velocity, shear rate, and particle concentration in the lower parts of the current, and sedimentation rate (e.g., Branney and Kokelaar 2002; Burgisser and Bergantz 2002; Sulpizio et al. 2007).

Branney and Kokelaar (2002) proposed that four intergradational end-member types of flow-boundary (direct-fallout-dominated, traction-dominated, granular flow-dominated and fluid-escape-dominated) account for the range of common lithofacies in ignimbrites. Each end-member type of

flow-boundary zone is characterised by distinctive velocity and concentration gradients, yet they are considered transitional into one another with changing rates of concentration, deposition and shear. The vertical succession of lithofacies within the deposit of a sustained current records the changing conditions and depositional processes with time (unsteadiness), while the lateral lithofacies variations along an entrachron record spatial variations during a single moment in time (non-uniformity, see Kneller and McCaffrey 1999; Choux and Druitt 2002; Branney and Kokelaar 2002).

Eruptive history and morphology of Las Cañadas volcano

Tenerife is composed of a large ignimbrite shield volcano, Las Cañadas volcano, constructed on coalesced and eroded basaltic shield volcanoes (Ancochea et al. 1990; 1999; Martí et al. 1994; Fig. 1). Numerous Plinian eruptions have occured in the past 2 Ma (Ancochea et al. 1990; Huertas et al. 2002; Brown et al. 2003; Dávila Harris, 2009; Dávila Harris et al. 2011). These deposited ignimbrites, and pumice and ash fall deposits across the island. The pyroclastic deposits are interleaved with numerous basaltic lavas from scattered monogenetic flank volcanoes, and from three volcanic rift-zones (Bryan et al. 1998a, b; Bryan et al. 2000; Pittari et al., 2006; Dávila Harris 2009; Dávila Harris et al. 2012). The southern flank of Las Cañadas volcano rises to 2.5 km above sea-level and drops abruptly back down to 0.5 km into the central caldera (Figs 1 and 2). For the purposes of this paper we consider that the southern flanks include a 180° sector that stretches from the north side of the Güimar valley to Guia de Isora in the west (Fig. 2). This southern flank is broadly concave, from steeper upper flanks (9–15°; Fig. 2) to lower gradient (<6°) coastal flanks (<200 m altitude; the Bandas del Sur) that reach as much as 5 km inland from the coast. The flank varies from 15–20 km wide. In detail, the lower gradient apron is not continuous and forms a coastal crescent that stretches from Los Cristianos in the west to just north of Poris de Abona. The eastern end of the southern flank of Tenerife is abruptly terminated by the partly filled Güimar collapse scarp, which is the result of one of several large sector-collapse landslides that have occurred on Tenerife over the past 2 Ma (Watts and Masson 2001; Dávila Harris et al. 2011).

The Bandas del Sur has a semi-arid climate prone to periodic flash floods, which have incised the slopes to produce a network of downhill-converging radial valleys. Palaeotopography indicates that the region has had a similar topography for the past 2 Ma (Pittari et al. 2006). Valleys and palaeo-valleys are 10–50 m deep, 10's to 100's of metres wide, and are separated by hundreds of metres-wide, flat-topped interfluves and narrower ridges (Fig. 1).

Terminology

We use pyroclastic density current (PDC) for any type of gaseous gravity current carrying pyroclastic material (i.e. including both 'fully-dilute' and 'granular fluid-based' types; Branney and Kokelaar 2002), and we use ignimbrite for the pumiceous deposit of a PDC (including ash-rich deposits). The term ignimbrite sheet is used to describe a succession of ignimbrites and subordinate fall deposits deposited during one eruption. We use the term valley-fill to describe those parts of the ignimbrite sheet deposited within valleys and the term veneer in a non-genetic sense, to describe topography-draping, thinner ignimbrite deposited on topographic highs (similar to 'overbank facies' of Schumacher and Schmincke 1990): no inference of deposition from the 'tail' of a PDC is implied (cf. IVDs of Walker et al. 1981). The term flow-unit is used to define an ignimbrite bounded by horizons (such as fall deposits, reworking, scours) that indicate pauses in current activity at that site. Lithofacies are summarised in Brown and Branney (2004a). We use the term entrachron to describe a cryptic surface within an ignimbrite that links together clasts that entered the current at the same time (e.g., a new type of juvenile material) and depochron to describe a cryptic surface that links together clasts that were deposited at the same time. We use the lithostratigraphic term 'member' for a lithologically-distinctive division that has regional distribution (see Brown and Branney 2004a): members do not necessarily correspond to individual flow-units.

Ignimbrite architecture of the Poris Formation

The 273 ka Poris Formation (Bryan et al. 1998a; Egdar et al. 2002; Brown et al. 2003; Brown and Branney 2004a) lies within the Quaternary Bandas del Sur Group of Tenerife (Fig. 2). It is a compound phonolite to tephri-phonolite ignimbrite sheet, composed of several ignimbrite flow-units with associated co-ignimbrite ash fall layers and pumice fall deposits emplaced during a Plinian eruption (Fig. 3). It outcrops in the Diego Hernandez sector of Las Cañadas' caldera wall (Edgar et al. 2002; Smith 2012) and along the southeast coast (Fig. 4; Bryan et al. 1998a; Edgar et al. 2002; Brown et al. 2004a). Proximal sections of the ignimbrite sheet are interpreted in Smith (2012). The present study focuses on the coastal ignimbrite sheet, which is widely 2–35 m thick and emplaced across a gently concave volcano flank cut by small dendritic valleys (10–40 m deep), separated by broad interfluves, which it variously draped and buried along a 50 km-long coastal strip (from Montaña Guaza near Los Christianos in the south, to El Baul in the northeast, Fig. 1).

The Poris Formation has been subdivided into eleven lithostratigraphic members and includes four ignimbrite flow-units (Fig. 3; Brown and Branney 2004a). Each of the four flow-units is separated by clear evidence for pauses in density current activity (e.g., pumice or ash fall layers, or eroded remnants of these). Flow-units 1–3 are composed mostly of massive lapilli-tuff within palaeovalleys and extensive ash layers across palaeo-ridges (Fig. 3). Flow-unit 4 is zoned, allowing it to be divided into four distinct lithostratigraphic members, and can be traced across the entire width of the Bandas del Sur (Fig. 4). Its compositional zoning has the form of compositional variations with height in the deposit, in the form of cryptic entrachrons that mark the entrances and exits of various distinctive components, including accretionary lapilli, abundant lithic clasts, and juvenile banded tephri-phonolite pumice clasts. However, there is no evidence within the flow-unit for the cessation of flow (i.e., no ash fall layers or reworking; see Brown and Branney 2004a). Moulds of allochthonous tree trunks are common in Flow-unit 4.

Distribution of ignimbrite flow-units of the Poris Formation

The distribution of each flow-unit varies considerably (Fig. 4). Flow-units 1 and 2 are restricted to a 10–20 km-wide zone in central parts of the Bandas del Sur (mostly between Tajao and Poris de Abona, Figs. 1 and 4). As they were the first ignimbrites to be emplaced they were thickest along valley axes, but the thickest valley fills have been eroded and the ignimbrites are preserved mostly as remnants along palaeo-valley sides and as centimetre-thick veneers over palaeo-ridges. The maximum preserved thicknesses are 2.6 m (Flow-unit 1 at Montaña Magua) and 2.2 m (Flow-unit 2). Flow-unit 3 outcrops between La Caleta and Montaña Magua (Fig. 1) and is preserved up to 93 cm thick in palaeo-valleys (between Tajao and La Caleta, Fig. 4).

Flow-unit 4 is much more extensive and overlaps all underlying flow-units (Fig. 4). Its outcrop width exceeds 37 km (between Aldea Blanca and Güimar; Figs 1 and 4). Internal entrachrons (marked by appearances and disappearances variously of accretionary lapilli, abundant lithic clasts, and tephri-phonolite pumice) reveal that the distribution of the current gradually increased with time (Fig. 4), and that later parts of the current (Member 9) entered the Güimar valley for the first time during the eruption. The flow-unit is thickest (>35 m) and most complete in central parts of the Bandas del Sur (e.g., La Caleta to Fasnia; Fig. 1). In the west it is generally thinner (<10 m) and only comprises later parts of Flow-unit 4 (Members 6–9) overlying Member 1 pumice and ashfall layers. In the East (Güimar valley, Fig 1) the ignimbrite sheet comprises only the latest parts (Member 9), locally with ashfall and pumice fall layers (Fig. 4). Ignimbrite is absent where the coastal flanks are steeper (between Fasnia and Güimar; Fig. 3).

Each ignimbrite flow-unit has an associated thin (cm-thick) co-ignimbrite ash fall layer. These ash layers are predominantly composed of ash pellets. They are more extensive than the ignimbrites, and covered much of the south coast of Tenerife (see Brown and Branney 2004a; Brown et al. 2010).

Longitudinal (parallel-to-current) architecture

The Poris ignimbrite sheet is absent on the steeper (9–15^{o}) upper flanks of Cañadas volcano, but is present locally in the caldera wall and on the nearby upper NE flank (Edgar et al. 2002; Smith 2012). More generally, the ignimbrites are preserved on the less steep (<4^{o}) slopes of the coastal pyroclastic apron (Fig. 3) within 5 km of the present coastline, but rarely above ~200 m altitude. The general absence of ignimbrite on the steeper (>4 ^{o}) slopes cannot be an artefact of subsequent erosion because (1) the enclosing fall deposits extend upslope beyond where the ignimbrites of the lower slopes pinch out; and (2) the architecture of the ignimbrite sheet shows that the original proximal edge of the ignimbrite is preserved on the lower gradient slopes (Fig. 5). The upper surfaces of the ignimbrite sheet generally dip 1–4º seaward, and the sheet pinches out up the broadly concave slope at 300–400 m altitude (Fig. 5).

The coastal apron provides excellent continuous 5 km-long longitudinal sections through the Poris ignimbrite sheet. Tracing the individual ignimbrite flow-units and the entrachrons within them in a downcurrent direction (see Fig. 5) has enabled the internal architecture to be reconstructed in a parallel-to-current orientation. This architecture is well illustrated in a ~1 km-long continuous section north-west of Montaña Magua (Fig. 5) where three ignimbrite flow-units (1, 2 and 4) are preserved in a current-parallel section both along a fossil interfluve and along a palaeo-valley. Both along the interfluve and along the valley axis, successive flow-units onlap in the upcurrent direction against the regional slope (Fig. 5): Flow-unit 1 thins upslope from 2 m to <0.06 m over a distance of ~100 m; Flow-unit 2 thins from 15 m to 2 m over the same distance (Fig. 5). Upslope, these flow-units pass into thin ash veneers that are texturally indistinguishable from the veneer deposits that they grade into laterally across palaeo-ridges (Fig. 5).

Flow-unit 4 also onlaps against the slope and thins from ~35 m (reconstructed thickness, Fig. 5) to 0 m upslope over a distance of <900 m. Entrachrons within it pick out similar internal retrogradational relationships with topography (Members 6-9 on Figs 5 and 6A-C). This onlapping, retrogradational architecture is repeated on a smaller scale producing a giant bedform in Flow-unit 4 at

Montaña Magua (Brown and Branney 2004b). Thus, the retrogradational geometry of the flow-units and their internal architectures mirrors the geometry of the entire ignimbrite sheet (Fig. 6D). The proximal edge of the ignimbrite sheet and all units within it have a 'feather edge' geometry (Fig. 6D; also exposed in quarry faces at El Arrecife). Similar onlapping retrogradational architectures are also seen in the Abades ignimbrite (Fig. 7F).

Tranverse (sideways-to-current) architecture: gradations from valley-fill to veneer facies

Lateral variations from thin veneers of ignimbrite on palaeo-ridges to thicker valley-fill ignimbrite in palaeo-valleys are well preserved. Several near-complete valley cross-sections are exposed at Montaña Magua, and we focus on these (Figs 1 and 7).

Flow-units 1 and 2

Near Montaña Magua the lower two flow-units each comprise an ignimbrite overlain by an extensive ash pellet fall layer (Figs. 3 and 7). Flow-unit 1 comprises up to 2.5 m thick, ash-rich yellowish lapilli-tuff with scattered accretionary lapilli. Flow-unit 2 comprises up to 15 m of poorly sorted massive lapilli-tuff, with local clast-supported pumice lenses along the palaeovalley sides. The ignimbrites are thickest in palaeovalleys, where they are lenticular in cross-section and flat topped (Fig. 7A-C). Moulds of small shrubs and current-orientated delicate twigs and grasses are commonly preserved along their bases. Complete gradations from valley-fill to veneer facies are exposed for flow-units 1 and 2 (Fig. 7). The ignimbrite veneers are laterally extensive across palaeo-ridges and are found on slopes as steep as 35°. They are typically several centimetres thick and are composed of massive tuff. Diffuse stratification is present at some localities. They locally thicken into shallow topographic depressions. The upper parts of both the valley-fill and veneer ignimbrites contain scattered accretionary lapilli and each ignimbrite flow-unit is overlain by an extensive, thin co-ignimbrite ash fall layer made of ash pellets (Brown and Branney 2004a; Brown et al. 2010; ash pellets are AP1 type of Brown et al. 2012).

Flow-unit 4

The lowermost part (Member 6) of Flow-unit 4 is geographically restricted with abundant large accretionary lapilli (Fig. 7). Within palaeovalleys it reaches 12 m thick and is massive. Diffuse bedding gradually appears within upper parts and towards palaeovalley margins, where initially indistinct, bedding gradually becomes more distinct and also more close-spaced, so that the massive valley-fill ignimbrite grades imperceptibly into the thinner, diffuse-stratified veneer facies (Fig. 7; this is 'splay-and-fade' stratification of Branney and Kokelaar 2002). The veneer component of Member 6 is complex with rapid lateral variations. It typically comprises a decimetre-thick unit of diffuse-bedded to stratified tuff and accretionary lapilli-rich lapilli-tuff with scattered pumice and lithic lapilli (see Brown et al. 2010; Fig. 7). Discontinuous planar scour surfaces separate beds, which lack accretionary lapilli in their lower portions. Low-angle cross-stratified tuff occurs locally at the base of these beds. Accretionary lapilli (AP2 types of Brown et al., 2012) are 10 times as abundant in the thin topography-draping veneer ignimbrite (~400–500/m^2) as they are in the coeval thicker, valley-filling ignimbrite (≤50/m^2). Elsewhere around Montaña Magua, the veneer ignimbrite exhibits stratification defined by discontinuous lenses and layers of lithic lapilli, pumice lapilli or accretionary lapilli. Small steep-sided scours are also present (see Brown and Branney 2004a).

Within Flow-unit 4, Member 6 passes up into Member 7 ignimbrite that lacks accretionary lapilli (Figs. 2 and 7). Within the palaeovalleys, Member 7 is >20 m-thick, homogenous massive lapilli-tuff. Laterally, this passes gradationally across palaeovalley sides into an extensive veneer ignimbrite, typically 2–5 m thick (Fig. 7). Within the veneer of Flow-unit 4, the contact between members 6 and 7 is sharp and marked by a scour surface. At many localities within the veneer, Member 7 includes stratified, cross-stratified, diffuse-bedded and massive lapilli-tuff. Subtle, complex vertical grading patterns (normal and inverse) of lithic and pumice lapilli are common. Individual beds and strata are discontinuous over metres to decimetres and it is not possible to trace them between outcrops. Pods, lenses and thin layers of clast-supported pumice or lithic lapilli and blocks are common throughout the veneer facies; in places they exhibit load-and-flame structures, some of which are

sheared in a downslope direction. Shallow to steep-sided and poly-phase scours and diffuse low-angle truncations that pass laterally into diffuse-bedding and then fade out laterally into massive lapilli-tuff are common ('scour splay-and-fade stratification' of Branney and Kokelaar 2002). A 9 m long by 0.4 m high dune bedform outcrops at Montaña Magua and was described in detail by Brown and Branney (2004b).

Member 7 passes up abruptly into Member 8, a widespread coarse-grained, clast-supported lithic-rich grey to pink ignimbrite that reaches 15 m-thick within palaeovalleys (Fig. 7). To the north of Montaña Magua it typically has a preserved thickness of 2–3 m and passes laterally into a 0.3–1 m-thick topography-draping veneer. It lacks the abundant lithic lapilli, blocks and boulders seen elsewhere in this member (see Brown and Branney 2004a). The juvenile pumice changes from highly vesicular phonolite to dense and variably vesicular, banded tephri-phonolite (Brown and Branney 2004a). The first appearance of the more mafic juvenile material can be traced throughout the ignimbrite sheet as an entrachron, as can the base of the lithic breccia, marked by the first appearance of abundant quantities of lithic clasts within the flow-unit. Metre-scale scouring of the underlying units has occurred locally (e.g. at Tajao, Fig. 1), but elsewhere the base exhibits spectacular load structures and pods into the underlying Member 7 ignimbrite. Member 8 passes gradationally upwards into Member 9 which is only preserved as a veneer facies pumiceous lapilli-tuff <1 m thick. It is commonly composed of clast-supported pumice lapilli and blocks. Its across-valley geometry and lithofacies transitions are not well constrained.

In summary, the ignimbrite flow-units are thick in palaeovalleys and thin over palaeo-ridges (Fig. 7D). The early flow units (1–3) thin markedly over palaeo-ridges, with thickness ratios of the order of 100:1. In contrast, the difference in thickness between coeval ignimbrite in palaeovalleys and palaeoridges in Flow-unit 4 is much less (<5:1; see Fig. 7D).

Interactions between density currents and topographic obstacles

Basaltic scoria cones up to 300 m high pepper the lower flanks of Las Cañadas volcano (see Bryan et al. 1998a; Kröchert and Buchner 2009; Fig. 8A). During explosive eruptions they obstructed PDCs and resulted in the upstream accumulation of anomalously thick sequences of ignimbrite. An instructive example of this can be seen in the Güimar valley (Fig. 1) — an 8 km wide, flat-bottomed scarp formed by catastrophic sector collapse of the SE flank of Tenerife. The Poris density currents flowed down the Guimar valley, and across two close-spaced scoria cones situated 1.5 km from the present coastline (Fig. 9). Long axes of imbricated tree moulds are aligned parallel to flow direction (towards the SE) and indicate that the current passed over the scoria cones (Fig. 9). However, Flow-unit 4 is anomalously thick between and upstream of the scoria cones: it is predominantly massive and exceeds 13 m in thickness immediately upstream of the northernmost scoria cone (Flow-unit 4, Fig. 9). It then thins to 3–6 m over the upstream sides of the scoria cones (logs B and D on Fig. 9). Yet, on flat ground downstream and laterally away from the cones, the density current apparently did not deposit anything, because the ignimbrite flow unit is absent there and the Poris Formation comprises only the ash fall and pumice fall layers (logs A and E on Fig. 9).

Another example of enhanced deposition of ignimbrite upstream of a cone is seen at the ~100 m-high Fasnia scoria cone (Fig. 8A). Here, massive ignimbrites of the Fasnia Formation exceed 7 m thick on the stoss side of the cone (Fig. 8B) while on the lee side the same ignimbrites are only a few centimetres thick and stratified, and they laterally pass into low-amplitude scour surfaces that cut the through underlying pumice fall deposits.

Discussion

Topography affected the extensive, radiating pyroclastic density currents (PDCs) on various different scales. These are discussed below.

Controls on the distribution of pyroclastic density currents

Differences between the distributions of the four ignimbrite flow-units (Fig. 4) are attributed to a combination of: (1) changing eruption dynamics; and (2) simultaneous depositional modification of the topography by the density currents. Although comparison of volume of each flow-unit is precluded by flow into the sea, the field relations strongly suggest that the volumes of the first three density currents were lower than those of the fourth current, resulting in Flow-units 1–3 having narrower geographic distributions. In addition, in-situ shrub moulds along the bases of Flow-units 1–3 indicate that these early currents had lower velocities, in contrast to the larger current that deposited Flow-unit 4, which was not only more laterally extensive and capable of transporting lithic blocks 15–20 km from source, but it also stripped mature forest from upper slopes, leaving widely scattered (allochthonous) tree moulds on the coastal plain. As the Poris eruption progressed, the valley/interfluve topography on the lower coastal flanks of Tenerife was gradually infilled by ignimbrite and, as a result, the later currents were less valley-confined (Figs. 5–7). We infer that this was the result of increasing overspill of small-volume PDCs from one valley into adjacent valleys.

During deposition of Flow-unit 4 the rapid increase in the geographic footprint of the density current (Fig. 4) in inferred to have resulted from increases in the mass-flux of the eruption (waxing flow) with a consequent increase in the volume of the density current. The rapid and marked lateral advance of the PDC across the region in eastwards and westwards directions, perpendicular to the flow-direction during the deposition of Flow-unit 4 (Fig. 4) also likely resulted from an increase in the volume of the density current during the climactic stages of the eruption. The current increased not only in capacity (the bulk mass of material carried) and spread out more, but its competence also increased, as recorded by the presence of abundant large lithic blocks and boulders in Member 8. Waxing flow, recorded by the upwards-coarsening, seems to have favoured widespread erosion and entrainment as recorded by the allochthonous tree trunks, lenses of locally-derived lithic clasts, and the presence of metre-scale scour surfaces in the deposits in Flow-unit 4 (Brown and Branney 2004a). Proximally, the increased eruptive mass-flux may also have favoured the current overtopping a broader stretch of the Las Cañadas caldera rim (Fig. 1).

Influence of regional-scale topography on deposition from PDCs

On a regional scale, deposition from the Poris density currents was strongly controlled by the large-scale morphology of the ignimbrite shield volcano. Geographic zones of contrasting PDC behaviour can be delineated along the southern flanks of Cañadas volcano (Fig. 10). Deposits in the most proximal regions (i.e., intra-caldera 1–5 km from source) are not available for study, but comparison with ancient dissected calderas suggests that thick accumulations of ignimbrite and lithic breccia were deposited from PDCs that were partially contained within caldera walls (e.g., the Ordovician Scafell Caldera, Lake District, Branney and Kokelaar 1994). Proximal parts of the ignimbrite sheet (<5 km from source) are preserved in the present caldera wall and reach 30 m thick, and are considered to have accumulated in a broad valley oriented east-west away from the caldera walls (Smith 2012).

In medial zones (>5–15 km from source, Fig. 10) the PCDs flowed away from the caldera down the steep upper flanks of Las Cañadas volcano. We infer from the absence of ignimbrite in these regions that the PDCs bypassed these steep slopes with accumulative to near-uniform flow capacity (e.g., Kneller and Branney 1995) and remained largely non-depositional for most of their passage to the sea.

In distal regions (>15 km from source; Fig. 10) the PDCs started to deposit, presumably caused by passage onto the more gentle (<6°) coastal slopes. We infer that the density currents deposited there as a result of depletive flow capacity (e.g., Kneller and Branney 1995); that is, the spatial decelerations incurred by flow across the regional concave slope. This, combined with the depletive effect of slightly divergent (radiating) flow paths around the island reduced the current's capacity to transport its particulate load, promoting deposition as the current encountered gradually less-steep slopes with proximity to the coast (Fig. 1). Similar processes have been demonstrated in laboratory experiments of aqueous density currents (Garcia and Parker 1989; Mulder and Alexander 2001; Kubo 2004), in numerical simulations (Kassem and Imran 2001) and, for example, where PDCs elsewhere crossed breaks-in-slope (e.g., Roobol et al. 1987; Giordano 1998; Macías et al. 1998; Sulpizio et al., 2007,

2010; Sulpizio and Dellino 2008). It is possible that the reduced gradient of the more coastal parts of the pyroclastic apron may have forced the current to undergo a downstream transition from supercritical to subcritical flow (e.g., hydraulic jump; Van Andel and Komar 1969), but this is not a requirement for deposition and is difficult to established from deposits (e.g. Gray et al. 2005). Turbulence can be generated at a hydraulic jump and this may promote substrate erosion and entrainment, and enhanced mixing with the ambient fluid (e.g., Komar 1971).

We note that scours of all scales occur within Flow-unit 4 deposits in areas where there is evidence for bypassing (i.e., the proximal edge of the coastal ignimbrite sheet, see Brown and Branney 2004a). This indicates that at these areas, substantive accelerations were close to neutral (bypassing with neither overall deposition nor erosion; Branney and Kokelaar 2002) such that relative minor fluctuations in the current (such as pulses or passage of eddies or roll waves) would have been sufficient to induce minor, ephemeral erosion and deposition.

The gradient between the caldera and the coast varies around the volcano. For example, locally on the SE flank, and widely around the north flank, the low-gradient coastal apron is absent, with steep slopes extending all the way to the sea (Figs. 1 and 2). Some of the shortest (14 km) and steepest (consistently $>9^{o}$) flanks on the southern side of the island occur between Fasnia and Güimar (Fig. 2). Poris ignimbrites are widely absent in this section, even at the coast. In this sector of Tenerife, the Poris PDCs bypassed all the way to the sea. We can deduce this because the fall deposits are present in the area and Poris ignimbrite is preserved proximally, directly upslope of this region in the Diego Hernandez caldera wall (Edgar et al. 2002; Smith 2012). We infer that the steeper coastal slopes in this region ensured that capacity of the PDCs remained uniform or accumulative and non-depositional all the way to the sea so that left little or no record was left of their passage.

The bypassing behaviour of the Poris PDCs across the flanks of Tenerife indicates that they were autosuspending currents in a near-equilibrium state (neither eroding nor depositing), similar to the behaviour of some turbidity currents in submarine channels (Stevenson et al. 2012). This condition exists where substantial accelerations approximate to zero (fig 1.1 of Branney and Kokelaar 2002), and

436 this, in turn, depends upon the interplay between any changes in mass flux at source (e.g. eruption
437 dynamics) and the particular configuration of the substrate slope. With a steady input at source, spatial
438 changes in slope induce spatial accelerations (accumulative flow) or decelerations (depletive flow) and
439 thus exert a primary control on the current dynamics and on whether the current erodes, bypasses or
440 deposits (e.g., Kneller and Branney 1995; Mulder and Alexander 2001; Brown and Branney 2004b;
441 refs in Sulpizio and Dellino 2008). The gentle slopes of the coastal pyroclastic apron on Tenerife are
442 composed of ignimbrite sheets, and is similar to turbidite fan systems constructed at the mouths of
443 submarine channels. Proximal scour-and-fill basin-facies turbidites deposited near the start of more
444 gentle slopes are inferred to result from currents that alternated between erosion and deposition (e.g.,
445 Kokelaar 1992; Amy et al. 2007) and are, we suggest, analogous to the proximal feather-edge of the
446 coastal Poris ignimbrite sheet.

447 Other ignimbrites in southern Tenerife show similar distributions, thinning and then pinching
448 out up the concave flank, and we suspect that all PDCs on Tenerife behaved in a similar manner to
449 those of the Poris eruption. Given that the Poris PDCs were depositing thick ignimbrite in proximal
450 extracaldera regions, and that runout distance is closely linked to sedimentation (Andrews and Manga
451 2012), we infer that passage down the long and steep slopes inhibited sedimentation in medial reaches
452 and increased the runout distances and the ignimbrite mass-loading on the coastal apron and offshore.

453 The internal onlapping architecture of the Poris ignimbrite sheet (Fig. 6D) means that the bases
454 of the flow-units, and also the base of the ignimbrite sheet as a whole (excluding the fall layers) are
455 diachronous. Each current did not commence deposition at the same time at all localities across the
456 region. Rather, the onset of deposition migrated upcurrent with time during passage of the current and
457 this advance continued until it reached what is now the proximal 'feather-edge' of each ignimbrite
458 flow-unit (Fig. 6D). This is particularly well illustrated by Flow-unit 4, which was deposited from a
459 sustained current that experienced several marked changes in the composition of clasts supplied to it
460 through time (e.g., Fig. 5). Entrachrons that enclose compositionally diverse units onlap against the
461 topography.

462 The complex onlap architecture is illustrated in more detail by the giant regressive bedform in
463 Member 8 (see Brown and Branney 2004b). It resulted from a sustained PDC that was just entering into
464 a region of deposition at that location. The diachronous character of the Poris ignimbrite sheet means
465 that individual vertical sections through the ignimbrite do not record the entire depositional history of
466 the parent PDC—the same holds true for each individual flow-unit. In general, the onlap relationships
467 suggest that a large proportion of the pyroclastic load of the PDCs was deposited at sea: there is a
468 substantial thickness of pyroclastic material offshore southern Tenerife (Bogaard 1998).
469 The architectural relationships in the Poris ignimbrite sheet resulted from unsteadiness and non-
470 uniformity in sustained density-stratified PDCs, and they are picked out by entrachrons. However, in
471 massive, homogenous ignimbrite sheets, such as are generated during super-eruptions, these
472 relationships may go unrecorded and the changing position of the aggradation surface during the
473 eruption will remain cryptic. Defining and tracing entrachrons in apparently homogeneous large-
474 volume (100–1000 km^3), ignimbrite sheets would be useful in understanding their emplacement
475 history, and may provide clues about the durations of sustained PDCs during cataclysmic eruptions.
476 Analysis of smaller-volume zoned ignimbrite sheets with well defined architectures, such as the Poris
477 ignimbrite, can provide critical clues to help in this endeavour.
478
479 **The interaction of PDCs with local topography**
480 The valley-fill to veneer lithofacies transitions in the Poris Formation ignimbrite flow-units (Fig. 7)
481 record changes in flow-boundary conditions laterally across topography, i.e., flow-boundary non-
482 uniformity. These differences are primarily the result of a density-stratified current interacting with
483 irregular topography (e.g., Valentine 1987; Pittari et al. 2006). Different topographic elevations project
484 into different levels within the current that have differing particle concentrations, turbulence intensities,
485 compositions (e.g., proportions of ash vs. pumice lapilli) and clast-support mechanisms. Thus, the
486 character of the lower flow-boundary zone that developed within the base of the current vary with
487 elevation.

In the lower flow-units (1–3), lateral transitions from thick massive lapilli-tuff (valley-fill facies) to thin tuff (veneer facies; Fig. 7) record deposition from strongly density-stratified pyroclastic currents that transported the majority of their coarse lapilli along valley axes. The thin ignimbrite veneers lack abundant pumice lapilli and indicate that higher levels (metres to tens-of-metres above the base) within the density-stratified current inundated the local topographic highs, but carried predominantly fine ash.

The marked veneer-to-valley-fill transitions in flow-units 1–3, are similar to those documented in the Oruanui ignimbrite, New Zealand (type B deposits of Wilson 2001). The thinness of the Oruanui veneer deposits was attributed to the 'fluidity' of the PDCs, helped by the presence of water in the substrate on the palaeo-valley walls (a 'hot-skillet' analogy), which is inferred to have promoted the downhill movement of coarse lapilli. However, coarse lapilli are absent in the Poris Formation on the wide, plateau-like interfluves, which suggests that the extensive upper levels of the Poris PDCs that travelled across the broad interfluves transported few coarse lapilli, in contrast to the current's lower, more concentrated levels that were more channelised along the valleys and evidently contained abundant coarse pumice. Steam-flashing of water in the substrate (Wilson 2001) would widely disrupt bedding, and is not recorded in the basal pumice fall layers of the Poris Formation. Moreover, the nature of the palaeosol and the spacing of in situ fossil shrubs indicate that the Poris deposits were emplaced in a dry desert landscape similar to that of the present day southern coast. The architectural relationships across palaeo-valleys (e.g. near Montaña Magua; Fig 1) allow some constraints to be placed on the thickness of the lowermost, more concentrated pumice lapilli-bearing levels of the currents at valley axes (Fig. 7). The lower, concentrated levels cannot have been thicker than the current depth of palaeovalleys or pumice and lithic lapilli would have been deposited widely upon the interfluves. We thus infer that lower, concentrated and lapilli-bearing levels of most of the density stratified current were probably less than several metres thick.

Insights into flow non-uniformity over topography can be gleaned by using the height in the deposit at which accretionary lapilli appear and disappear as time-lines. Evidence from numerous

ignimbrite sheets on Tenerife indicated that accretionary lapilli initially nucleated in the form of small ash pellets within the buoyant atmospheric co-ignimbrite ash plumes (Brown et al. 2010). These pellets fell out into the current over both valleys and topographic highs and were eventually deposited within the ignimbrite. Additional layers of fine ash accreted to the pellets during their passage through the co-ignimbrite-density current system transforming the ash pellets into accretionary lapilli (Brown et al. 2010; also see Van Eaton and Wilson 2012). It is known that they fell directly into the lower parts of the Flow-unit 4 current rather than having been carried from proximal locations by the current because, pumice lapilli and lithic lapilli of pneumatic equivalence to the accretionary lapilli are abundant in the valley-fill ignimbrites, but they are absent in the thin ash veneers, which also contain the accretionary lapilli. Clearly, the competence of the current (measure of the largest-size clast a current is able to transport) on interfluves was insufficient to transport lapilli-sized clasts, and yet the veneer ignimbrites nevertheless contain abundant accretionary lapilli. At Montaña Magua, depochrons marking the appearance and disappearance of accretionary lapilli in Flow-unit 4 are ~0.6 m apart in veneer ignimbrite, but they are more than 12 metres apart in adjacent coeval massive valley-fill ignimbrite (Fig. 7). This indicates that depositional aggradation rates were ~20 times greater in the valleys than on the ridges. However, assuming that accretionary lapilli fell out of upper parts of the current into the aggrading ignimbrite across valleys and ridges, then there is a discrepancy between the thickness ratio of valley-fill and veneer ignimbrite (~1:20) and the accretionary lapilli concentration ratio (1:10). This can be accounted for by the common scours in veneer ignimbrite that indicate intermittent erosion. Thus, while ignimbrite was aggrading within valleys, ignimbrite on the interfluves underwent periodic deposition and erosion by the current.

The lateral variations in lithofacies between valley-fill and veneer ignimbrites exhibited by later deposited parts of Flow-unit 4 (Members 7–9; Fig. 7D) are considerably less marked than those exhibited by the earlier flow-units. This change was the result of: (A) a reduction in the relief and accommodation space provided by the valleys due to partial filling by the earlier ignimbrite flow-units; and (B) a marked increase in the volume of the fourth PDC. The increase in volume meant that the

remaining topographic relief provided by the interfluves between the partly filled valleys failed to penetrate so high into the now thicker current's density-stratification, such that the more concentrated (granular fluid) lower levels of the current flowed more extensively across the interfluves. Nevertheless, particle concentrations in the lower levels of the current on the interfluves were not sufficiently high to entirely suppress turbulence, as recorded by diffuse bedding and stratification in the veneer facies of Member 7, in contrast with the entirely massive fills in the valleys. Conservation of mass requires that lateral spreading of the current across interfluves would affect the concentration-profile of the current at those locations, for example with thinning of the granular-fluid in lowermost levels of the current. Thus, the character of the lower flow-boundary zone of the current may have changed laterally with fluid-escape dominated deposition along the valleys, to form the massive lapilli-tuff at valley axes, and with less steady deposition more affected by granular flow and tractional processes across the interfluves, as recorded by the more variable, variously diffuse-stratified veneers (e.g., Branney and Kokelaar 2002).

Similar lateral variations in a large density current are recorded in the ignimbrite sheet of the 1991 eruption of Mount Pinatubo, Philippines (Scott et al. 1996), which also inundated radiating valleys and broad interfluves.

Depositional records of bypassing currents: sediment traps on the flanks of Las Cañadas volcano

Enhanced deposition from density currents on the stoss-side of topographic obstructions is common (e.g. Bursik and Woods 2000) and results from local decelerations, in some cases accompanied by the development of upstream propagating bores within the blocked, lower parts of density stratified currents (see Bursik and Woods 2000). The local current decelerations (depletive flow) will locally decrease the flow capacity. On southern flanks of Tenerife, thick ignimbrite accumulations developed upstream of scoria cones, which acted as 'sediment traps'. We infer that the high-concentration basal parts of the current were forced to slow, pond and flow around the sides of the cone (e.g., Baines 1995; Bursik and Woods 2000), while higher, less dense and turbulent levels of the current decoupled (sensu

566 Fisher 1995) and flowed across the cone, eroding the substrate, bypassing, or depositing thin ash
567 veneers on the lee side.

568 In the broad Güimar valley, ignimbrite is absent within the Poris Formation on flat ground away
569 from the scoria cones (logs A and E on Fig. 9). Either the Poris PDC did not flow across these regions
570 or it remained non-depositional and bypassed where not blocked by topographic obstacles. However,
571 the local presence of ignimbrite upstream of several scoria cones indicates that the density current
572 accelerated down the steep east-facing scarps of the valley (>35° 1600 m high, Fig. 9) and then fanned
573 out across the valley bottom. Across most of the valley floor the current remained non-depositional
574 (logs A and E on Fig. 9) and passed out to sea. The current here deposited ignimbrite only where it was
575 forced to slow and flow around scoria cones. Bypassing of PDCs over short distances (<5 km) is
576 common on steep-sided composite volcanoes (e.g., Mount Misery, St. Kitts, Robool et al. 1987; Mount
577 Pinatubo, Philippines, Scott et al. 1996; Roccamonfina volcano, Italy, Giordano 1998). Bypassing over
578 greater distances (> 30 km) is rarer but was inferred to have occurred during large-magnitude eruptions
579 such as the Campanian Ignimbrite, Italy (Fisher et al. 1993). During hazard surveys it would seem
580 appropriate to target scoria cones or other traps on potential bypass surfaces in order to search for local
581 ignimbrite accumulations that would record the passage of large currents: this could help construct
582 eruption histories and determine the hazards around large explosive volcanoes.
583

584 **Using longitudinal ignimbrite architecture to understand large-scale eruption dynamics**

585 Longitudinal architectures in ignimbrite sheets are useful for deciphering large-scale eruption dynamics
586 and regional-scale PDC behaviour (De Rita et al. 1998; Branney and Kokelaar 2002). Two conceptual
587 models have been proposed to account for retrogradation architectures in ignimbrite sheets (Branney
588 and Kokelaar 2002): (1) extending aggradation with dual onlap, such as may result from waxing flow,
589 or (2) overall retrogradation, such as may result when runout distance decreases during waning flow
590 (Fig. 11A). In the former model, the geographic area of deposition increases with time, creating onlap
591 architectures in proximal areas mirrored by onlap in more distal areas; and may result from overall

592 waxing flow. In the latter model, onlap upslope in proximal areas is accompanied by offlap in distal
593 areas as the distal limit of deposition decreases with time, recording a gradual decrease in runout
594 distance with time, such as may occur due to overall waning flow conditions. The distal architecture of
595 the Poris ignimbrite sheet is obscured by the sea, but from subaerial exposures alone it is apparent that
596 neither of these models fits perfectly. This is because the field relations indicate that retrogradation
597 occurred during strongly waxing flow (see Fig. 5, 6 and 11B; see also Brown and Branney 2004b), as
598 indicated by the overall upward-coarsening sequence, from tuff at the base of Flow-unit 1 to lithic
599 breccias high in Flow-unit 4, (thought to record peak flow conditions as the caldera subsided), and also
600 by the overall increase in geographic area covered by the currents with time. The lower flow-units (1-3)
601 are geographically restricted and preserve in-situ fossil shrubs at their bases, whereas Flow-unit 4 is
602 more widespread and contains abundant allochthonous tree trunks and entrained locally-derived lithic
603 clasts, and coarsens upward into an extensive lithic breccia (see Brown and Branney 2004b). These
604 features suggest that the capacity, competence and the dynamic pressure of the current increased with
605 time during the Poris eruption. The lithic breccia high in Flow-unit 4 is a particularly widespread unit
606 and probably records peak flow conditions (Brown and Branney 2004a). Thus, the retrogradational
607 architecture that is widely exhibited within the Poris ignimbrite sheet across southern Tenerife was
608 assembled during predominantly waxing flow conditions.
609 We propose that where the current flowed onto lower slopes it was critically balanced with
610 respect to deposition: that is, substantive accelerations within the current were close to zero
611 (autosuspension) because the waxing mass-flux of the current was balanced by depletive flow on the
612 gentle concave slope. In this condition even a very small change in topography was sufficient to locally
613 push the current into deposition (substantive deceleration). Thus, rather minor slope-changes induced
614 slight spatial decelerations sufficient to trigger the onset of deposition in a restricted (~50 m reach)
615 depositional zone. Downcurrent of this zone, the slope was unchanged and the current bypassed to the
616 ocean. Soon, however, the location of the minor slope-induced deposition shifted upcurrent because the
617 current now had to flow over the newly formed ≤5 m-thick lens of deposit. Downslope of the lens crest

618 the current continued to flow away downslope to the ocean, without depositing (bypassing). The new
619 deposit lens now itself caused the local deceleration (depletive flow) causing the zone of deposition to
620 shift sourceward, depositing a new lens and so on, so that over time (hours) a single, extensive layer
621 (2–5 m thick over interfluves and <20 m thick along valley axes) was gradually assembled
622 retrogradationally during the eruption. As the eruption waxed, new additions to this layer were coarser-
623 grained (e.g. lithic breccia). Thus we infer that the retrogradation exhibited widely by the Poris and
624 other ignimbrite sheets in southern Tenerife resulted from the gentle concave regional slope and not
625 due to waning flow.
626 Rates of deposition on this gentle concave slope remained low when compared with the inferred
627 larger volumes of material that passed by. This is in contrast with more rapid deposition at a marked
628 break-of-slope as described elsewhere where wholesale rapid deposition is caused by abrupt
629 deceleration with or without a hydraulic jump at a steep obstacle or major change in slope. Eventually,
630 as flow peaked the zone of deposition broadened with aggradation of a new layer of lithic breccia
631 overlapping the earlier retrogradational components of the sheet (Fig. 11C). Locally, the peak waxing
632 phase was sufficient to cause erosion and entrainment of just-deposited ignimbrite, stripping up to 4 m
633 of just-deposited ignimbrites).
634 The presence of a widespread clast-supported pumice-rich ignimbrite (Member 9, Fig. 3)
635 capping Flow-unit 4 is consistent with retrogradation of the ignimbrite sheet, this time as the eruption
636 waned after the caldera-collapse climax. These pumice concentrations are thought to have formed when
637 buoyant large pumice clasts overpassed to become deposited near the distal limits of the current,
638 leaving typical clast-supported pumice-accumulations (snouts and levees). During the sustained
639 current's waning, the distal limits of the current retracted sourceward (retrogradation), producing a
640 strand-line of pumice deposits preserved in uppermost parts of the resultant ignimbrite sheet. This
641 mechanism accounts for upper pumice concentrations in zoned ignimbrites elsewhere (e.g. Zaragoza
642 ignimbrite, Carrasco-Nuñez and Branney 2005). The last upslope lens deposited during final waning
643 stages of the current left a 2-m high dam that after the eruption collected water forming a small lake in

644 which 2 m of pumiceous sediments accumulated (Branney and Brown 2004a), showing that the
645 upslope limit of the present ignimbrite sheet represents the true preserved original limit, not an eroded
646 remnant.

647 In summary, the longitudinal retrogradational architecture of the onshore Poris ignimbrite sheet
648 (see Fig. 11C) resulted primarily from the gently concave regional slope, and occurred during both
649 overall waxing flow conditions (coarsening upwards) and during late-stage waning flow conditions
650 (recorded by upper lithic-poor pumice accumulations). As the last, more prolonged current waxed to
651 the climactic phase, earlier-deposited parts of the ignimbrite were locally stripped out by vigorous
652 erosion, and during the climactic phase of the current (as the caldera collapsed; Brown and Branney
653 2004a) a second layer of ignimbrite was widely assembled above the earlier, retrogradational part of
654 the ignimbrite. This layer was characterised by widespread lithic breccias.
655

656 ## Conclusions

657 Cryptic internal architectures within an extensive ignimbrite sheet on Tenerife have revealed how
658 conditions within a widespread, sustained PDC varied spatially (due to the influence of the regional
659 slope and local valleys and obstacles) and with time (as a result of changing eruption dynamics and
660 modification of topography by deposition). During a large Plinian eruption four widespread, sustained
661 pyroclastic density currents swept down the broadly concave flanks of Las Cañadas volcano.

662 (1) The overall gentle concavity of the volcano's flanks controlled where the currents deposited on
663 a regional scale. The currents bypassed the steeper upper flanks and began to deposit as the
664 slopes gradually decreased with proximity to the coast, more than 15 km from the source
665 caldera. Deposition occurred during both waxing and waning flow periods, and so is inferred to
666 have resulted predominantly from topography-induced spatial deceleration (depletive flow)
667 caused by the combination of slightly divergent flow (flow-paths fanning out) and passage onto
668 lower gradients.

(2) Bypassing (flow without deposition) characterised PDC behaviour for the majority of the runout distance. The flanks of Cañadas volcano behaved as a broad ‘chute’ or bypass surface, conveying most of the erupted material to the ocean, more than 15 km from source. Such PDC behaviour has two consequences: (A) the volume of the ignimbrite eruptions on Tenerife is difficult to estimate because the bulk of the material resides offshore, so eruption volumes far exceed the volumes of onshore deposits; and (B) it is liable to lead to under-estimates of the number of hazardous density currents to have passed across a volcano flank, because such currents widely leave no depositional record of their passage. Thus, to estimate the true number of density currents that have crossed an area requires careful piecing-together of incomplete information from scattered patches of deposit. This is unlikely to be achieved where exposure is less superlative than is the case in the southern Tenerife desert.

(3) The prolonged nature (and hence large volume) of a pyroclastic density current that was sustained, for example, throughout the entire duration of a caldera-collapse phase of a large explosive eruption (e.g. Poris Flow-unit 4) may not be immediately apparent from a deceptively thin ignimbrite flow-unit. The thinness of the ignimbrite on a gently concave volcano flank is the result of limited accommodation space (topography), not the duration or size of the current, which may have been prolonged. At any one location deposition occurred during just a fraction of the flow’s duration across that location.

(4) On gently concave slopes, ignimbrite flow-units were assembled incrementally by upslope advance of the deposit’s source-facing feather-edge. The deposition was diachronous, and the resultant retrogradational onlap architecture within the ignimbrite flow-unit is developed both within the valley fills and in the thin ignimbrite veneers. However, whereas in the veneers, this architecture can be apparent from diffuse-bedding with low-angle backset-type geometry, the same architecture can be entirely cryptic within massive, thicker valley-filling ignimbrite, and only revealed there by analysis of the compositional zoning.

(5) Local obstacles, such as scoria cones on the bypass surface acted as sediment traps by inducing local depletive conditions with consequent localised deposition of ignimbrite from currents that left little record elsewhere. When attempting fieldwork reconstructions of the PDC history of a large explosive volcano, targeting of stoss sides of scoria cones for investigation is a rewarding strategy

(6) Deposition of ignimbrite by a sustained PDC modifies the substrate topography sufficiently rapidly to alter the current's spatial patterns of deposition and erosion. In hazard models that predict density current dispersals, assumptions of a constant (e.g. DEM) topography during an eruption may yield misleading results in the case of sustained currents.

(7) The Poris PDCs were concentrated (granular-fluid based) and density-stratified, as revealed by the field relations across the margins of flow-parallel valleys. Lower, granular-fluid levels of the earlier, smaller currents were largely channelled within pre-existing valleys, whereas higher, more dilute levels spilled widely across extensive interfluves, leaving finer-grained veneers. In contrast, the larger current that deposited Flow-unit 4 flowed across a landscape in which topographic irregularities had been substantially dampened by deposition of ignimbrite from the earlier PDCs. The lower, granular-fluid levels of this current flowed widely across both valleys and interfluves, although the competence of the current to transport large clasts was somewhat higher along valley axes than it was along the elevated interfluves. This PDC was sustained before, during, and after the climactic caldera collapse phase of the eruption, and its grainsize variations record the waxing flow, peak flow, and waning flow conditions. Topography-induced depletive flow was locally sufficiently marked to induce deposition even during the initial phase of waxing flow. However, at several locations the current eroded and entrained several metres thickness of loose ignimbrite deposited by the same current earlier during its waxing phase. This widespread removal of lower parts of Flow-unit 4 means that many sections are incomplete, and record just peak flow and subsequent phases of the current.

719 The presented data illustrate how variations in PDC dispersal, onlapping relationships, diachronous
720 surfaces, bypassing and the waxing and waning of individual currents and of the eruption overall mean
721 that any single vertical section through an ignimbrite sheet may record just a fraction of the complete
722 eruption sequence. Failure to recognise this during hazard assessments may lead to under-estimations
723 of PDC volumes, dispersals and frequencies. This may be most critical on ocean island volcanoes
724 where subaerial flanks act as bypass surfaces across which the PCDs convey the majority of their load
725 into the sea. However, where exposure is sufficient, and by targeting local sediment traps such as stoss
726 sides of scoria cones, more complete flow-histories can be carefully pieced together from patchy
727 deposits, particularly where reconstructions are aided by compositional zoning of the ignimbrite.
728

729 ## Acknowledgements

730 We thank Natasha Smith, Peter Kokelaar, Pablo Dávila-Harris, Steve Self and Jan Zalasiewicz for
731 many useful discussions. We thank Brittany Brand and Roberto Sulpizio for critical reviews that
732 greatly improved the manuscript and Michael Manga for reviews and editorship.
733

734 ## References

735 Alexander J, Morris M (1994) Observations on experimental, non-channelized, high-concentration
736 turbidity currents and variations in deposits around obstacles. J Sed Res A64:899-909
737
738 Allen SR, Cas RAF (1998) Lateral variations within coarse co-ignimbrite lithic breccias of the Kos
739 Plateau Tuff, Greece: Bull Volcanol 59:356-377
740
741 Amy LA, Kneller BC, McCaffrey WD (2007) Facies architecture of the Grès de Peïra cava, SE France:
742 Landward stacking patterns in ponded turbidite basins. J Geol Soc 164:143-162
743

744 Ancochea E, Fuster JM, Ibarrola E, Cendrero A, Coello J, Hernan F, Cantagrel JM, Jamond C (1990)
745 Volcanic evolution of the island of Tenerife (Canary Islands) in the light of new K-Ar data: J Volcanol
746 Geotherm Res 44:231-249
747
748 Ancochea E, Huertas MJ, Cantagrel JM, Coello J, Fuster JM, Arnuad N, Ibarrola E (1999) Evolution of
749 the Cañadas edifice and its implications for the origin of the Cañadas Caldera (Tenerife, Canary
750 Islands): J Volcanol Geotherm Res 88:177-199
751
752 Andrews GDM, Branney MJ (2011) Emplacement and rheomorphic deformation of a large, lava-like
753 rhyolite ignimbrite: Grey's Landing, southern Idaho. Geol Soc Am Bull 123:725-743
754
755 Andrews BJ, Manga M (2011) Effects of topography on pyroclastic density current runout and
756 formation of co-ignimbrites. Geology 39:1099-102
757
758 Andrews BJ, Manga M (2012) Experimental study of turbulence, sedimentation, and co-ignimbrite
759 mass partitioning in dilute pyroclastic density currents. J Volcanol Geotherm Res 225-226:30-44
760
761 Baines PG (1995) Topographic effects on stratified flows. Cambridge University Press, 482 pp
762
763 Best JL, Kostaschuk RA, Peakall J, Villard PV, Franklin M (2005) Whole flow field dynamics and
764 velocity pulsing within natural sediment-laden underflows. Geology 33:765-768
765
766 Bogaard P (1998) $^{40}Ar/^{39}Ar$ ages of Pliocene-Pleistocene fallout tephra units and volcaniclastic deposits
767 in the sedimentary aprons of Gran Canaria and Tenerife (sites 953, 954 and 956). Proc Ocean Drilling
768 Program, Sci Res 157:329-41.
769

770 Bourdier J, Abdurachman EK (2001) Decoupling of small-volume pyroclastic flows and related
771 hazards at Merapi volcano, Indonesia. Bull Volcanol 63:309-325
772
773 Branney MJ, Kokelaar BP (1992) A reappraisal of ignimbrite emplacement: progressive aggradation
774 and changes from particulate to non-particulate flow during emplacement of high-grade ignimbrite.
775 Bull Volcanol 54:504-520
776
777 Branney MJ, Kokelaar BP (1994) Volcanotectonic faulting, soft-state deformation and rheomorphism
778 of tuffs during development of a piecemeal caldera, English Lake District. Geol Soc Am Bull 109:507-
779 530
780
781 Branney MJ, Kokelaar BP (1997) Giant bed from a sustained catastrophic density current flowing over
782 topography: Acatlan ignimbrite, Mexico. Geology 25:115-118
783
784 Branney MJ, Kokelaar P (2002) Pyroclastic density currents and the sedimentation of ignimbrites. Geol
785 Soc London Memoir 27:1-152
786
787 Branney MJ, Barry TL, Godchaux M (2004) Sheathfolds in rheomorphic ignimbrites. Bull Volc
788 66:485-491
789
790 Brown RJ, Barry TL, Branney MJ, Pringle MS, Bryan SE (2003) The Quaternary pyroclastic
791 succession of southern Tenerife, Canary Islands: explosive eruptions, related subsidence and sector
792 collapse. Geol Mag 140:265-288
793
794 Brown RJ, Branney MJ (2004a) Event-stratigraphy of a caldera-forming ignimbrite eruption on
795 Tenerife: the 273 ka Poris Formation. Bull Volcanol 66:392-416

796

797 Brown RJ, Branney MJ, (2004b) Bypassing and diachronous deposition from pyroclastic density
798 currents: evidence from a giant regressive bedform (Poris Formation, Tenerife). Geology 32:445-448
799

800 Brown RJ, Branney MJ, Maher C, Dávila-Harris P (2010) Origin of accretionary lapilli within ground-
801 hugging density currents: Evidence from pyroclastic couplets on Tenerife. Bull Geol Soc Am 122:305-
802 320
803

804 Brown RJ, Bonadonna C, Durant AJ (2012) A review of ash aggregation. Phys Chem Earth 45-46:65-
805 78
806

807 Bryan SE, Marti J, Cas RAF (1998a) Stratigraphy of the Bandas del Sur Formation: an extracaldera
808 record of Quaternary phonolitic explosive volcanism from the Las Cañadas edifice, Tenerife (Canary
809 Islands). Geol Mag 135:605-636
810

811 Bryan SE, Marti J, Cas RAF (1998b) Lithic breccias in intermediate volume phonolitic ignimbrites,
812 Tenerife (Canary Islands): constraints on pyroclastic flow depositional processes. J Volcanol Geotherm
813 Res 81:269-296
814

815 Bryan SE, Marti J, Cas RAF, Marti J (2000) The 0.57 Ma Plinian eruption of the Granadilla Member,
816 Tenerife (Canary Islands): an example of complexity in eruption dynamics and evolution. J Volcanol
817 Geotherm Res 103:209-238
818

819 Burgisser A, Bergantz GW (2002) Reconciling pyroclastic flow and surge: The multiphase physics of
820 pyroclastic density currents. Earth Planet Sci Lett 202:405-418
821

822 Bursik MI, Woods AW (2000) The effects of topography on sedimentation from particle-laden
823 turbulent density currents. J Sed Res 70: 53-63
824
825 Calder ES, Cole PD, Dade WB, Druitt TH, Hoblitt RP, Huppert HE, Ritchie L, Sparks RSJ, Young SR
826 (1999) Mobility of pyroclastic flows and surges at the Soufriere Hills Volcano, Montserrat. Geophys
827 Res Lett 26:537-540
828
829 Carrasco-Núñez G, Branney MJ (2005) Progressive assembly of a massive layer of ignimbrite with
830 normal-to-reverse compositional zoning: the Zaragoza ignimbrite of central Mexico. Bull Volcanol 68:
831 3-20
832
833 Choux CM, Druitt TH (2002) Analogue study of particle segregation in PDCs, with implications for
834 the emplacement mechanisms of large ignimbrites. Sedimentology 49:907-928
835
836 Dade WB, Huppert HE (1996) Emplacement of the Taupo ignimbrite by a dilute, turbulent flow:
837 Nature 381:509-512
838
839 Dávila Harris P (2009) Explosive ocean-island volcanism: the 1.8–0.7 Ma explosive eruption history of
840 Cañadas volcano recorded by the pyroclastic successions around Adeje and Abona, southern Tenerife,
841 Canary Islands. Unpub PhD thesis, Univ Leics, UK
842
843 Dávila Harris P, Branney MJ, Storey M (2011) Large eruption-triggered ocean-island landslide at
844 Tenerife: Onshore record and long-term effects on hazardous pyroclastic dispersal. Geology 39:951-
845 954
846

847 Dávila Harris P, Ellis BS, Branney MJ, Carrasco-Nunez G (in press) Physical volcanology and
848 geochemistry of a vitric spatter-bearing ignimbrite: the Quaternary Adeje Formation, Cañadas volcano,
849 Tenerife. Bull Volcanol
850
851 Dellino et al., 2007. 2010
852
853 Denlinger RP, Iverson RM (2001) Flow of variably fluidized granular masses across three dimensional
854 terrain, 2. Numerical predictions and experimental texts. J Geophys Res 106:553-566
855
856 De Rita D, Giordano G, Milli S (1998) Forestepping-backstepping stacking patterns of volcaniclastic
857 successions: Roccamonfina volcano, Italy. J Volcanol Geotherm Res 80:155-178
858
859 Doronzo DM, Valentine GA, Dellino P, de Tullio MD (2010) Numerical analysis of the effect of
860 topography on deposition from dilute pyroclastic density currents. Earth Planet Sci Lett 300:164-73
861
862 Doronzo DM, Dellino (2012) Interaction between pyroclastic density currents and buildings:
863 Numerical simulation and first experiments. Earth Planet Sci Lett 310:286-292
864
865 Druitt TH (1998) Pyroclastic density currents: In: Gilbert JS, Sparks RSJ (Eds) The Physics of
866 explosive eruptions. Geol Soc London Spec Pub 145:145-182
867
868 Druitt TH, Calder E, Cole PD, Hoblitt RP, Loughlin S, Norton GE, Ritchie LJ, Sparks RSJ, Voight B
869 (2002) Small-volume, highly mobile pyroclastic flows formed by rapid sedimentation from pyroclastic
870 surges at Soufriere Hills Volcano, Montserrat: an important volcanic hazard. In: Druitt TH, Kokelaar
871 BP (Eds) The eruption of Soufrière Hills Volcano, Montserrat. Geol Soc London Memoir 21:263-279
872

873 Dufek J, Wexler J, Manga M (2009) Transport capacity of pyroclastic density currents: Experiments
874 and models of substrate-flow interaction. J Geophys Res 11:DOI: 10.1029/2008JB006216
875
876 Edgar CJ, Wolff JA, Nichols HJ, Cas CAF, Marti J (2002) A complex quaternary ignimbrite-forming
877 phonolite eruption: the Poris Member of the Diego Hernandez Formation (Tenerife, Canary Islands): J
878 Volcanol Geotherm Res 118:99-130
879
880 Fierstein J, Hildreth W (1992) The Plinian eruptions of 1912 at Novarupta, Katmai National Park,
881 Alaska. Bull Volcanol 54:646-684
882
883 Fierstein J, Wilson CJN (2005) Assembling an ignimbrite: Compositionally defined eruptive packages
884 in the 1912 Valley of Ten Thousand Smokes ignimbrite, Alaska. Bull Geol Soc Am 117:1094-1107
885
886 Fisher RV (1966) Mechanism of deposition from pyroclastic flows. Am J Sci 264:350-363
887
888 Fisher RV (1990) Transport and deposition of a pyroclastic surge across an area of high relief – the 18
889 May 1980 eruption of Mount St. Helens, Washington. Geol Soc Am Bull 102:1038-1054
890
891 Fisher RV, Orsi G, Ort M, Heiken G (1993) Mobility of a large-volume pyroclastic flow –
892 emplacement of the Campanian ignimbrite, Italy. J Volcanol Geotherm Res 56:205-220
893
894 Fisher RV (1995) Decoupling of pyroclastic currents - hazards assessment: J Volcanol Geotherm Res
895 66:257-263
896
897 Garcia MH, Parker G (1989) Experiments on hydraulic jumps in turbidity currents near a canyon-fan
898 transition. Science 245:393-396

Gertisser R, Cassidy NJ, Charbonnier SJ (2012) Overbank block-and-ash flow deposits and the impact of valley-derived, unconfined flows on populated areas at Merapi volcano, Java, Indonesia. Nat Haz 60:623-648

Giordano G (1998) Facies characteristics and magma-water interaction of the White Trachytic Tuffs (Roccamonfina Volcano, Southern Italy). Bull Volcanol 60:10-26

Girolami L, Roche O, Druitt TH, Corpetti T (2010) Velocity fields and depositional processes in laboratory ash flows. Bull Volcanol72:747-759, doi:10.1007/s00445-010-0356-9

Gray TE, Alexander J, Leeder MR (2005) Quantifying velocity and turbulence structure in depositing sustained turbidity currents across breaks in slope. Sedimentology 54:467-488 dpi 10.1111/j.1365-3091.2005.00705.x

Gurioli L, Sulpizio R, Cioni R, Sbrana A, Santacroce R, Luperini W, Andronico D (2010) Pyroclastic flow hazard assessment at Somma-Vesuvius based on geological record. Bull Volcanol 72:1021-1038

Hiscott RN (1994) Loss of capacity, not competence, as the fundamental process governing deposition from turbidity currents. J Sed Res 64:209-214

Huertas MJ, Arnaud NO, Ancochea E, Cantagrel JM, Fúster JM (2002) $^{40}Ar/^{39}Ar$ stratigraphy of pyroclastic units from the Cañadas volcanic edifice (Tenerife, Canary Islands) and their bearing on the structural evolution. J Volcanol Geotherm Res 115:351-365

924 Kassem A, Imran J (2001) Simulation of turbid underflows generated by the plunging of a river.
925 Geology 29:655-659
926
927 Kneller B, Edwards D, McCaffrey W, Moore R (1991) Oblique reflection of turbidity currents.
928 Geology 19:250-252
929
930 Kneller B, Branney MJ (1995) Sustained high-density turbidity currents and the deposition of thick
931 massive sands. Sedimentology 42:607-617
932
933 Kneller B, McCaffrey W (1999) Depositional effects of flow non-uniformity and stratification within
934 turbidity currents approaching a bounding slope: Deflection, reflection, and facies variation. J Sed Res
935 69:980-991
936
937 Kokelaar P (1992) Ordovician marine volcanic and sedimentary record of rifting and volcanotectonics.
938 Snowdon, Wales, United Kingdom. Bull Geol Soc Am 104:1433-1455
939
940 Komar PD (1971) Hydraulic jumps in turbidity currents. Geol Soc Am Bull 82:1477-1488
941
942 Kröchert J, Buchner E (2009) Age distribution of cinder cones within the Bandas del Sur formation,
943 southern Tenerife, Canary Islands. Geol Mag146:161-172
944
945 Kubo Y (2004) Experimental and numerical study of topographic effects on deposition from two-
946 dimensional, particle-driven density currents. Sediment Geol 164:311-26.
947
948 Legros F, Kelfoun K (2000) On the ability of pyroclastic flows to scale topographic obstacles. J
949 Volcanol Geotherm Res 98:235-241

950

951 Lirer L, Petrosino P, Alberico I, Postiglione I (2001) Long-term volcanic hazard forecasts based on
952 Somma-Vesuvio past eruptive activity. Bull Volcanol 63:45-60

953

954 Loughlin SC, Calder ES, Clarke A, Cole PD, Luckett R, Mangan MT, Pyle DM, Sparks RSJ, Voight B,
955 Watts RB (2002) Pyroclastic flows and surges generated by the 25 June 1997 dome collapse, Soufrière
956 Hills volcano, Montserrat. In: Druitt TH, Kokelaar BP (Eds) The eruption of Soufrière Hills Volcano,
957 Montserrat. Geol Soc London Memoir 21:181-209

958

959 Lube G, Cronin SJ, Thouret JC, Surono (2011) Kinematic characteristics of pyroclastic density currents
960 at Merapi and controls on their avulsion from natural and engineered channels. Geol Soc Am Bull
961 123:1127-1140

962

963 Macías JL, Espíndola JM, Bursik M, Sheridan MF (1998) Development of lithic-breccias in the 1982
964 pyroclastic flow deposits of El Chichón volcano, Mexico. J Volcanol Geotherm Res 83:173-196

965

966 Morris SA, Alexander J (2003) Changes in flow direction at a point caused by obstacles during passage
967 of a density current. J Sediment Res 73:621-629

968

969 Marti J, Mitjavila J, Arana V (1994) Stratigraphy, structure and geochronology of the Las Cañadas
970 caldera (Tenerife, Canary Islands) Geol Mag 131:715-727

971

972 Mulder T, Alexander J (2001) Abrupt change in slope causes variation in the deposit thickness of
973 concentrated particle-driven density currents. Mar Geol 175:221-235

974

975 Pittari A, Cas RAF, Edgar CJ, Nichols HJ, Wolff JA, Marti J (2006) The influence of
976 palaeotopography on facies architecture and pyroclastic flow processes of a lithic-rich ignimbrite in a
977 high gradient setting: The Abrigo ignimbrite, Tenerife, Canary Islands. J Volcanol Geotherm Res
978 152:273-315
979
980 Robool MJ, Smith AL, Wright JV (1987) Lithic breccias in pyroclastic flow deposits on St. Kitts, West
981 Indies. Bull Volcanol 49:694-707
982
983 Roche O, Gilbertson MA, Phillips JC, Sparks RSJ (2005) Inviscid behaviour of fines-rich pyroclastic
984 flows inferred from experiments on gas-particles mixtures. Earth Planet Sci Lett 240:401-414
985 doi:10.1016/j.epsl.2005.09.053.
986
987 Roche O, Atalli, M, Mangeney A, Lucas A (2011) On the run-out distance of geophysical gravitational
988 flows: insight from fluidized granular collapse experiments. Earth Planet Sci Lett 311:375-385, doi:
989 10.1016/j.epsl.2011.09.023
990
991 Roche O (2012) Depositional processes and gas pore pressure in pyroclastic flows: an experimental
992 perspective. Bull Volcanol 74:1807-1820, doi: 10.1007/s00445-012-0639-4
993
994 Rossano S, Mastroloronzo G, De Natale G (2004) Numerical simulation of pyroclastic density currents
995 on Campi Flegrei topography: a tool for statistical hazard estimation. J Volcanol Geotherm Res 132:1-
996 14
997
998 Schumacher R, Schmincke H-U (1990) The lateral facies of ignimbrites at Laacher See volcano. Bull
999 Volcanol 52:271-285
1000

1001 Scott WE, Hoblitt RP, Torres RC, Self S, Martinez ML, Nillos TJ (1996) Pyroclastic flows of the June
1002 15 1991, climactic eruption of Mount Pinatubo. In: Newhall CG, Punongbayan S (Eds) Fire and Mud:
1003 eruptions of Pinatubo, Philippines. Philippine Institute of Volcanology and Seismology, Quenzen City.
1004 University of Washington Press, Seattle, 545-570
1005
1006 Smith N (2012) Near-vent processes of the 273 ka Poris eruption (Tenerife). Unpublished PhD Thesis, Univ
1007 Liverpool
1008
1009 Sohn YK (1997) On traction-carpet sedimentation. J Sed Res 67:502-509
1010
1011 Stevenson CJ, Talling PJ, Wynn RB, Masson DG, Hunt JE, Frenz M, Akhmetzhanhov A, Cronin BT
1012 (2013) The flows that left no trace: very large-volume turbidity currents that bypassed sediment
1013 through submarine channels without eroding the sea floor. Mar Pet Geol 41:186-205
1014
1015 Sulpizio R, Mele D, Dellino P, La Volpe L (2007) Deposits and physical properties of pyroclastic
1016 density currents during complex Subplinian eruptions: the AD 472 (Pollena) eruption of Somma
1017 Vesuvius, Italy. Sedimentology 54:607-635
1018
1019 Sulpizio R, Dellino P (2008) Sedimentology, depositional mechanisms and pulsating behaviour of
1020 pyroclastic density currents. In: Gottsmann J, Marti J, (Eds) Caldera volcanism: analysis, modelling
1021 and response. Developments in Volcanology 10:57-96, Elsevier, Amsterdam
1022
1023 Sulpizio R, De Rosa R, Donato P (2008) The influence of variable topography on the depositional
1024 behaviour of pyroclastic density currents: The examples of the Upper Pollena eruption (Salina Island,
1025 southern Italy). J Volcanol Geotherm Res 175:367-385
1026

1027 Sulpizio R, Bonasia R, Dellino O, Mele D, Di Vito MA, La Volpe L (2010) The Pomici di Avellino
1028 eruption of Somma-Vesuvius (3.0 ka BP). Part II: sedimentology and physical volcanology of
1029 pyroclastic density current deposits. Bull Volcanol 72:559-577
1030
1031 Valentine GA (1987) Stratified flow in pyroclastic surges. Bull Volcanol 49:616-630
1032
1033 Valentine GA, Wohletz KH, Kieffer SW (1992) Effects of topography on facies and compositional
1034 zonation in caldera-related ignimbrites: Geol Soc Am Bull 104:154-165
1035
1036 Van Andel TH, Komar PD (1969) Ponded sediments of the Mid-Atlantic ridge between 22 and 23
1037 North. Geol Soc Am Bull 80:1163-1190
1038
1039 Van Eaton AR, Wilson CJN (2013) The nature, origins and distribution of ash aggregates in a large-
1040 scale wet eruption deposit: Oruanui, New Zealand. J Volcanol Geotherm Res 250:129-154
1041
1042 Walker GPL, Wilson CJN, Froggatt PC (1981) An ignimbrite veneer deposit—the trail marker of a
1043 pyroclastic flow. J Volcanol Geotherm Res 9:409–421
1044
1045 Watts AB, Masson DG (2001) New sonar evidence for recent catastrophic collapses of the north flank
1046 of Tenerife, canary islands. Bull Volcanol 63:8-19
1047
1048 Wilson CJN, Walker GPL (1985) The Taupo Eruption, New Zealand: II. The Taupo Ignimbrite. Phil
1049 Trans Roy Soc London, Series A-Math Phys Eng Sci 314:229-310
1050
1051 Wilson CJN (2001) the 26.5 ka Oruanui eruption, New Zealand: an introduction and overview. J
1052 Volcanol Geotherm Res 112:133-174

Woods AW, Bursik MI, Kurbatov AV (1998) The interaction of ash flows with ridges. Bull Volcanol 60:38-51

Figure Captions

Figure 1. Map of south Tenerife with the major outcrops of the Poris Formation marked. Delineated areas refer to regions referred to in later figures. DEM from GRAFCAN (www.grafcan.es).

Figure 2. DEM of Tenerife shaded for slope angle. Note the crescent-shaped region of low gradient slopes along the southern coast where most of the Poris ignimbrites were deposited (the Bandas del Sur region). Inset shows representative slope profiles as marked on map.

Figure 3. Generalised and composite vertical section of the Poris Formation as exposed along the southern coast of Tenerife with summary of the main characteristics of the members. Taken from Brown and Branney (2004b). L – lapillistone; LT – lapilli tuff; acc – accretionary lapilli; pel - ash pellets; p – pumice-rich; l – lithic-rich; m – massive; db – diffuse-bedded; s – stratified; xs – cross-stratified. See Brown and Branney (2004b) for a full description of members and lithofacies.

Figure 4. Distribution of ignimbrite flow-units across the southern flank of Tenerife. Representative measured sections through the Poris Formation illustrating the distribution and thickness variations of flow-units. Inset DEM of Tenerife showing the minimum areas of the island inundated by successive PDCs. The dispersal of PDCs increased with time during the eruption. Cartoon illustrating the dispersal of the four flow-units in the Poris Formation (see Fig. 1 for localities).

Figure 5. Parallel-to-current architecture of the Poris ignimbrite sheet at Montaña Magua (Fig. 1). Measured sections through the ignimbrite sheet indicate that the flow-units, and members in Flow-unit 4, pinch-out upslope against the substrate. Thus the base of the ignimbrite sheet is diachronous. Logs compressed for clarity: inset shows the location of measured sections and a restored longitudinal cross-section through the ignimbrite sheet.

Figure 6. Longitudinal architecture of the Poris ignimbrite sheet around Montaña Magua (see Fig 1 and inset in Fig 5). A) View downcurrent of Member 8 (Flow-unit 4) which onlaps upstream against the topographic slope (UTM: 357661/3119160). Member 7 (also of Flow-unit 4) in distance and preserved in small topographic depressions (arrowed). B) Member 7 pinching out upslope (UTM: 357945/3119059). C) Opposite side of valley to B. Bedding within Member 7 ignimbrite pinching out against the topographic slope. Current is from left to right. D) Lens of Member 9 ignimbrite overlain by volcaniclastic sands and gravels that were deposited against the upstream-dipping surface of the ignimbrite sheet. E) Member 8 lithic breccia forming the proximal feather edge of the ignimbrite sheet at El Arrecife. All lower units have pinched out further downslope. Current oblique out of page, left to right (UTM: 357654/3117857). F) Block diagram illustrating the reconstructed architecture of the ignimbrite sheet as based on outcrops around Montaña Magua (see Figs 5 and 7). Note the onlapping relationships of successive units and the retro-gradational, back-stepping architecture. F) Parallel-to-current section through the Abades ignimbrite showing onlapping of lithic-bearing layers (dashed lines) against the palaeoslope (arrowed). The base of the ignimbrite sheet is diachronous.

Figure 7. Representative logs at Montaña Magua through the ignimbrite sheet in veneer, valley-margin and valley-fill locations (for location see inset, Fig. 5). A) Panoramic view of spectacular palaeo-valley-filling ignimbrites. View to north and current out of page. Palaeo-valley axis runs out of the centre of the page (see inset in Fig. 5 for location). B) Close-up of northern valley-fill in B showing transition from valley-filling facies to veneer facies. Position of logs in A is indicated. Note that these

outcrops are being progressively covered by bulldozed rubble from adjacent construction work. C) Close-up of southern valley-fill in B showing abrupt pinch-out of valley-fill facies in Flow-unit 2. Flow-unit 2 was largely confined within the valley. D) Cartoon showing reconstructed transverse-to-current architecture across a palaeo-valley. Lithofacies as in Fig. 1 and Brown and Branney (2004b).

Figure 8. Interaction of PDCs with scoria cones on the southern flank of Tenerife. A) Photo of the Fasnia scoria cone (Fig. 1; UTM 359476/3123344), which has an anomalously stoss-side accumulation of Fasnia Formation ignimbrite; lee side is mantled by coeval thin ignimbrites and fall deposits. B) Anomalously thick ignimbrite on stoss side of Fasnia cone.

Figure 9. The interaction of PDCs and scoria cones in the Poris Formation. A) Measured sections through the Poris ignimbrite sheet in the Güimar valley (see inset for localities). Ignimbrite sheet is composed mostly of Flow-unit 4, which is thickest immediately upstream of the scoria cones, but is absent in localities away from the cones. PDCs generated in Las Cañadas caldera flowed into the Güimar valley on their way to the sea. Insets show location of sections. Aerial photograph 2011 Google ©.

Figure 10. Cartoon illustrating the different depositional regimes developed as PDCs disperse away from Las Cañadas caldera on Tenerife. In intra-caldera settings high ignimbrite accumulation rates resulted from topographic reflection and obstruction of PDCs by the growing caldera wall (A). In immediate extracaldera settings parts of the PDC that escaped the caldera rapidly sedimented thick ignimbrite over flat ground (B; see Smith and Kokelaar submitted). As the currents accelerated down the steep upper flanks of the flanks of the volcano they entered into an accumulative capacity and started to erode the substrate (C). They were effectively in a bypassing regime. Ignimbrite was not deposited except where parts of the current were obstructed by scoria cones (D). As they reached the lower flanks the currents passed onto lower gradient slopes, decelerated and entered into a depletive

capacity. This may have coincided with a hydraulic jump in the current. Loss of capacity resulted in ignimbrite deposition. The transition from a bypassing regime into a depositional regime is marked in the deposit by abundant stratification and scours within the deposit (E). Deceleration across the coastal flanks and out into the ocean resulted in rapid sedimentation rates (F).

Figure 11. Conceptual models for the architecture of the Poris ignimbrite sheet on the southern flank of Tenerife and interpretations of the gross eruption dynamics (following Branney and Kokelaar 2002). A) Two possible models to explain the genesis of the observed retrogradational, onlapping architecture of the proximal edge of the Ignimbrite sheet: extending aggradation with dual onlap (waxing mass-flux) or retrogradation (strongly waning flow). B) Cartoon qualitatively illustrating the changing mass flux of the Poris PDCs as deduced from lithological evidence in the ignimbrites. C) Preferred interpretation of the Poris ignimbrite sheet as inferred from both architecture and from lithological evidence—extending aggradational with dual onlap followed by retrogradation architecture resulted from an initial intermittent but low volume that increased rapidly during the eruption before strongly waning.

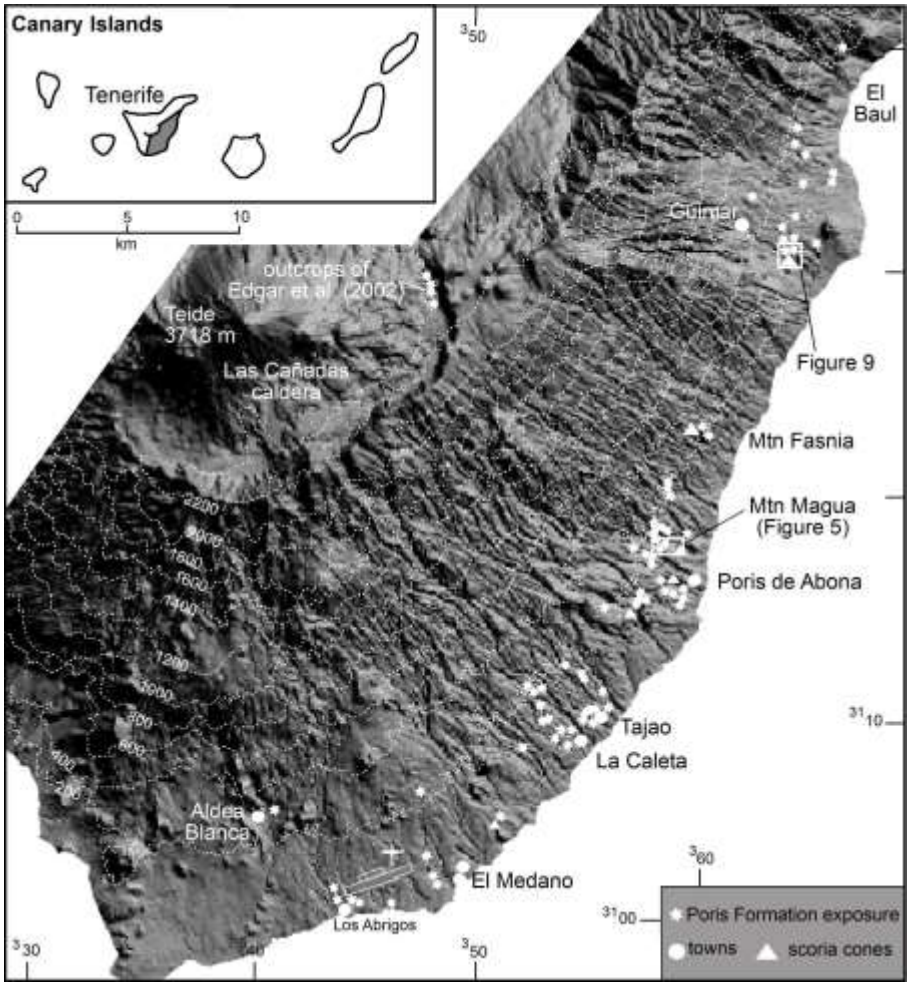
Canary Islands
Tenerife
0
5
10
km
3 50
El Baul
Güimar
outcrops of Edgar et al. (2002)
Teide 3718 m
Las Cañadas caldera
Figure 9
Mtn Fasnia
Mtn Magua (Figure 5)
Poris de Abona
2200
2000
1800
1600
1400
1200
1000
800
600
400
200
Tajao
La Caleta
31 10
Aldea Blanca
El Medano
Los Abrigos
3 60
31 00
3 30
40
3 50
Poris Formation exposure
towns
scoria cones

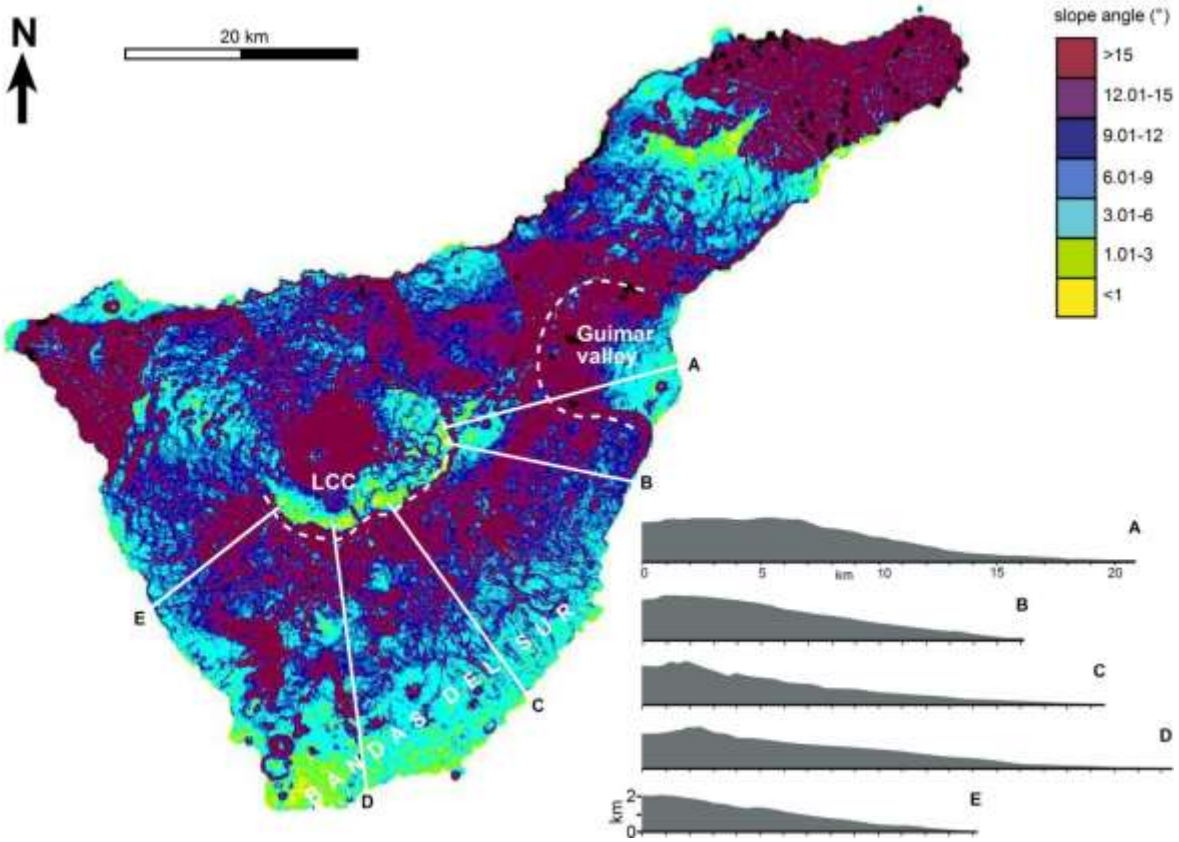
N
20 km
slope angle (°)
>15
12.01-15
9.01-12
6.01-9
3.01-6
1.01-3
<1
Guimar valley
LCC
A
B
C
D
E
RANDA DEL SUR
km
0
5
10
15
20
2
1
0

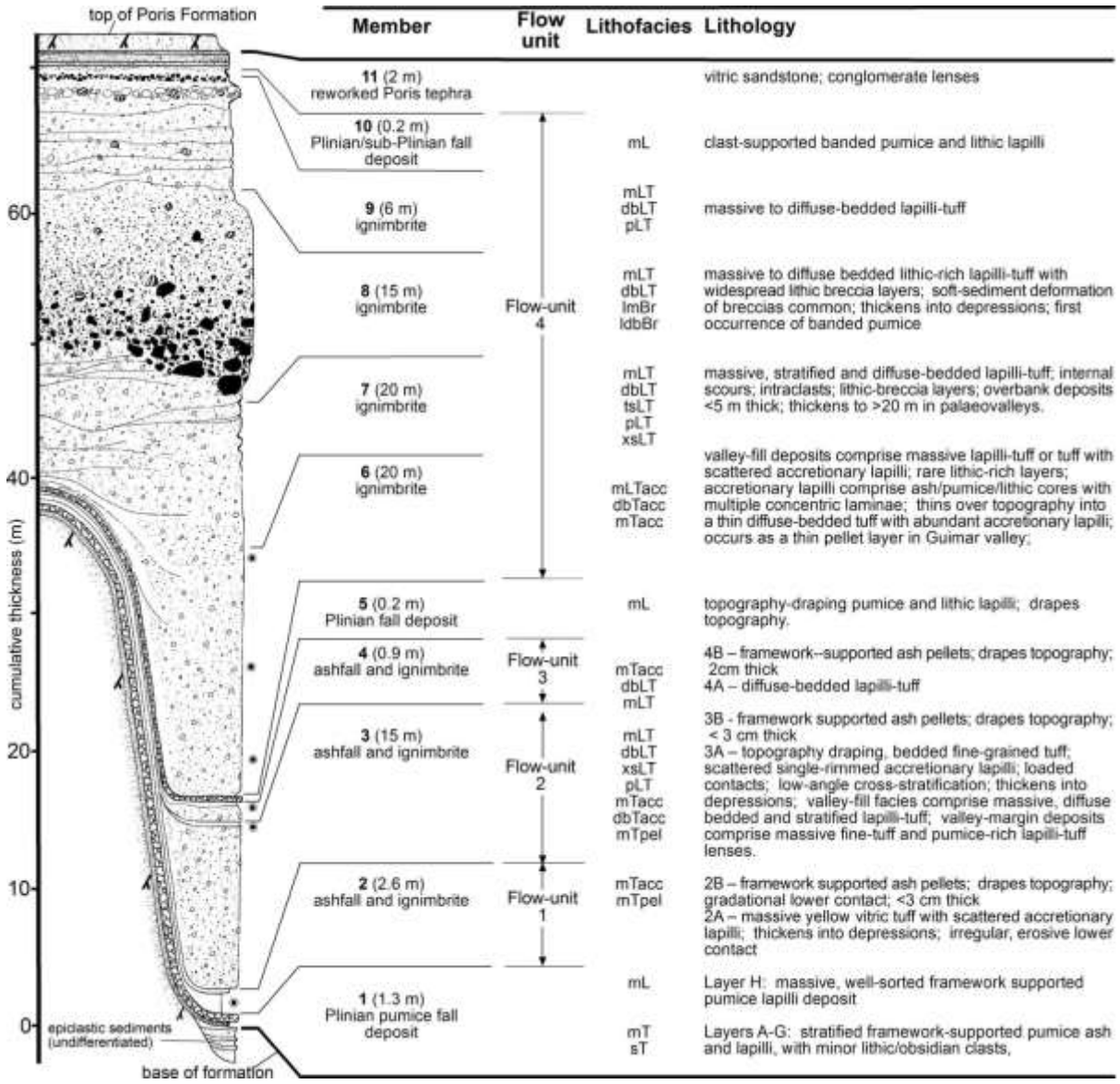
top of Poris Formation
cumulative thickness (m)
0
10
20
40
60
epiclastic sediments (undifferentiated)
base of formation
Member
Flow unit
Lithofacies
Lithology
11 (2 m) reworked Poris tephra
vitric sandstone; conglomerate lenses
10 (0.2 m) Plinian/sub-Plinian fall deposit
mL
clast-supported banded pumice and lithic lapilli
9 (6 m) ignimbrite
mLT
dbLT
pLT
massive to diffuse-bedded lapilli-tuff
8 (15 m) ignimbrite
Flow-unit 4
mLT
dbLT
lmBr
ldbBr
massive to diffuse bedded lithic-rich lapilli-tuff with widespread lithic breccia layers; soft-sediment deformation of breccias common; thickens into depressions; first occurrence of banded pumice
7 (20 m) ignimbrite
mLT
dbLT
tsLT
pLT
xsLT
massive, stratified and diffuse-bedded lapilli-tuff; internal scours; intraclasts; lithic-breccia layers; overbank deposits <5 m thick; thickens to >20 m in palaeovalleys.
6 (20 m) ignimbrite
mLTacc
dbTacc
mTacc
valley-fill deposits comprise massive lapilli-tuff or tuff with scattered accretionary lapilli; rare lithic-rich layers; accretionary lapilli comprise ash/pumice/lithic cores with multiple concentric laminae; thins over topography into a thin diffuse-bedded tuff with abundant accretionary lapilli; occurs as a thin pellet layer in Guimar valley;
5 (0.2 m) Plinian fall deposit
mL
topography-draping pumice and lithic lapilli; drapes topography.
4 (0.9 m) ashfall and ignimbrite
Flow-unit 3
mTacc
dbLT
mLT
4B – framework--supported ash pellets; drapes topography; 2cm thick
4A – diffuse-bedded lapilli-tuff
3 (15 m) ashfall and ignimbrite
Flow-unit 2
mLT
dbLT
xsLT
pLT
mTacc
dbTacc
mTpel
3B - framework supported ash pellets; drapes topography; < 3 cm thick
3A – topography draping, bedded fine-grained tuff; scattered single-rimmed accretionary lapilli; loaded contacts; low-angle cross-stratification; thickens into depressions; valley-fill facies comprise massive, diffuse bedded and stratified lapilli-tuff; valley-margin deposits comprise massive fine-tuff and pumice-rich lapilli-tuff lenses.
2 (2.6 m) ashfall and ignimbrite
Flow-unit 1
mTacc
mTpel
2B – framework supported ash pellets; drapes topography; gradational lower contact; <3 cm thick
2A – massive yellow vitric tuff with scattered accretionary lapilli; thickens into depressions; irregular, erosive lower contact
1 (1.3 m) Plinian pumice fall deposit
mL
Layer H: massive, well-sorted framework supported pumice lapilli deposit
mT
sT
Layers A-G: stratified framework-supported pumice ash and lapilli, with minor lithic/obsidian clasts,

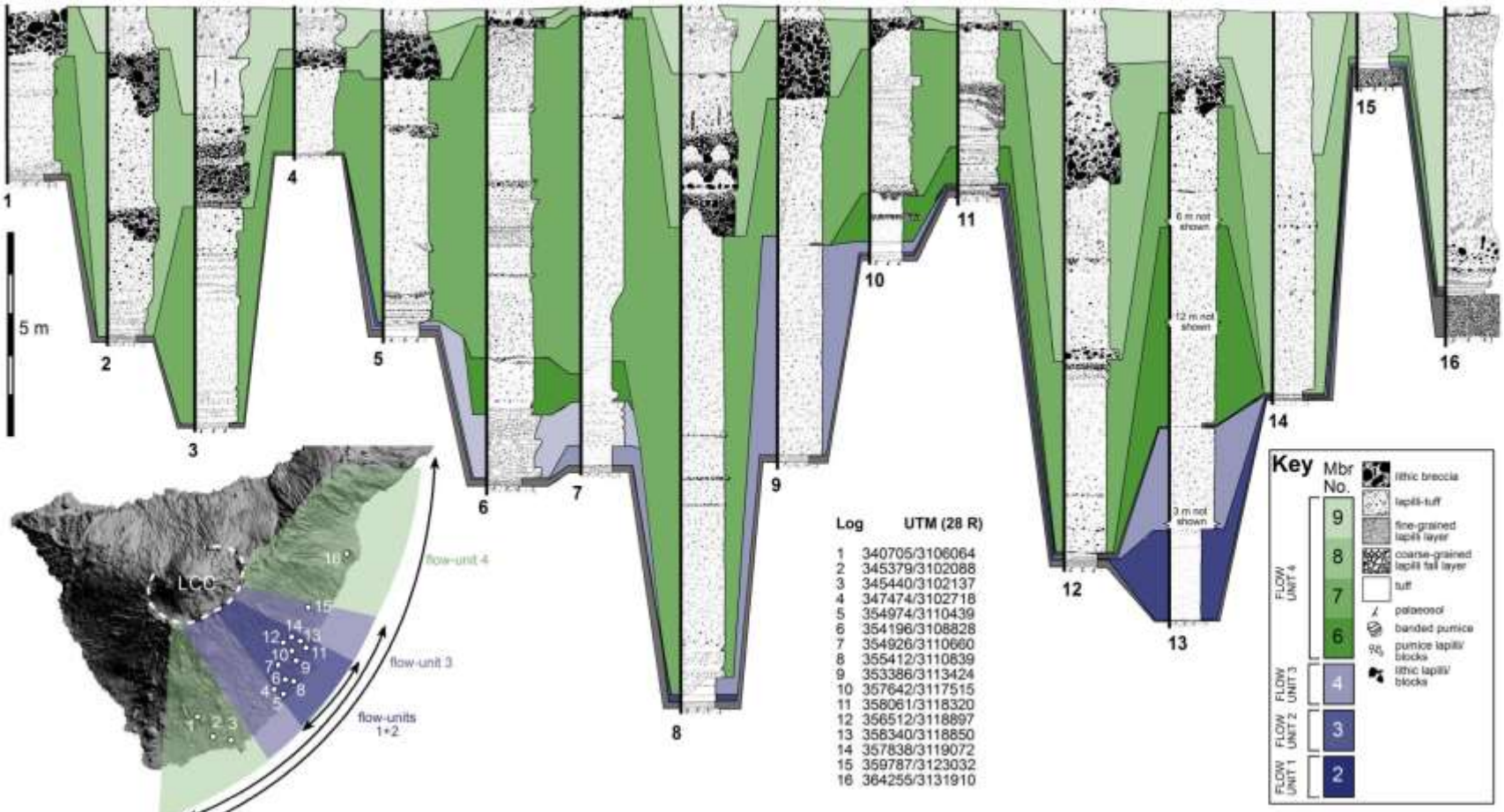
5 m
1
2
3
4
5
6
7
8
9
10
11
12
13
14
15
16
6 m not shown
12 m not shown
3 m not shown
LCC
flow-unit 4
flow-unit 3
flow-units 1+2
Log UTM (28 R)
1 340705/3106064
2 345379/3102088
3 345440/3102137
4 347474/3102718
5 354974/3110439
6 354196/3108828
7 354926/3110660
8 355412/3110839
9 353386/3113424
10 357642/3117515
11 358061/3118320
12 356512/3118897
13 358340/3118850
14 357838/3119072
15 359787/3123032
16 364255/3131910
Key
Mbr No.
FLOW UNIT 4
FLOW UNIT 3
FLOW UNIT 2
FLOW UNIT 1
lithic breccia
lapilli-tuff
fine-grained lapilli layer
coarse-grained lapilli fall layer
tuff
palaeosol
banded pumice
pumice lapilli/ blocks
lithic lapilli/ blocks

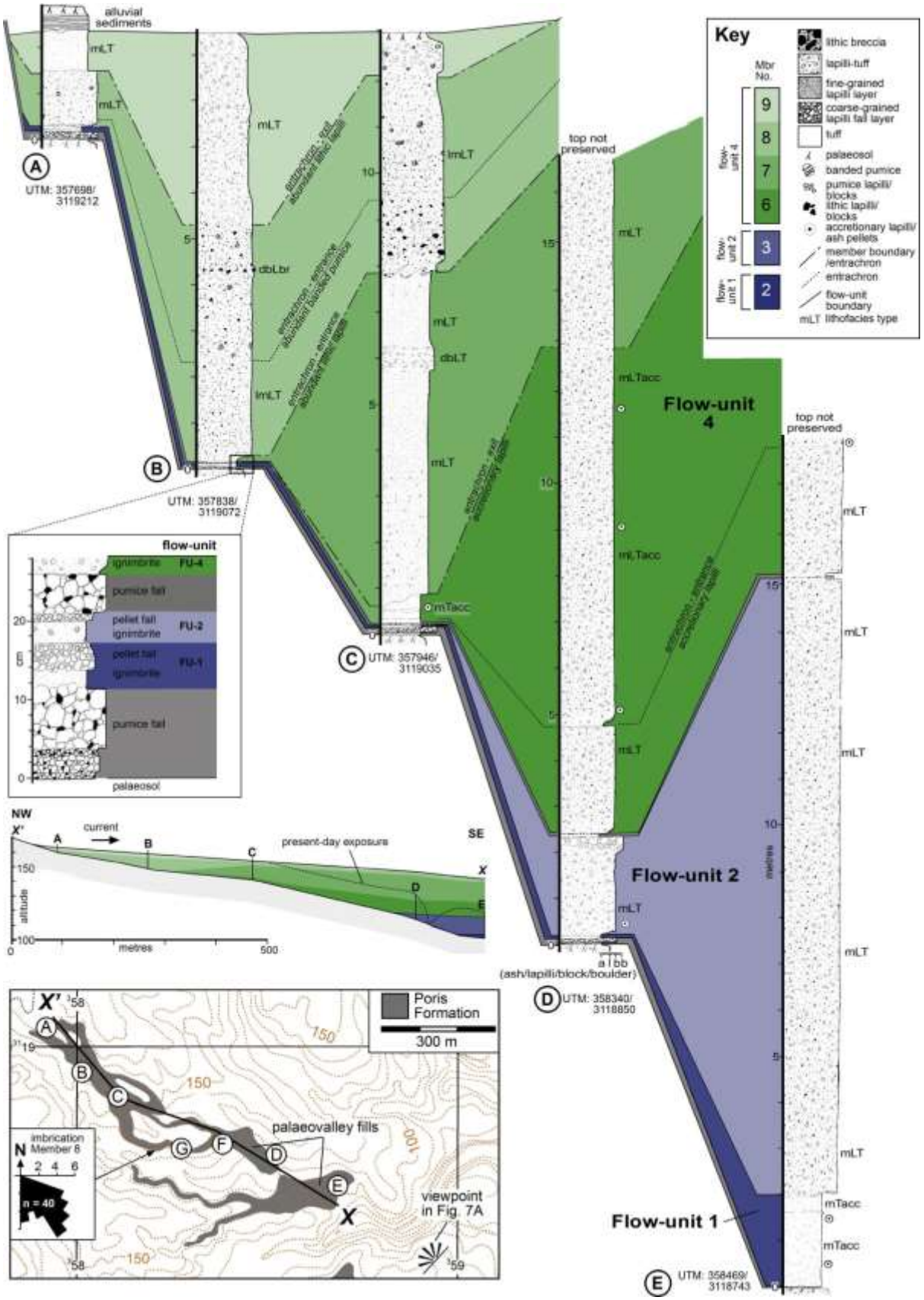
Key
Mbr No.
flow-unit 4
flow-unit 2
flow-unit 1
9
8
7
6
3
2
lithic breccia
lapilli-tuff
fine-grained lapilli layer
coarse-grained lapilli fall layer
tuff
palaeosol
banded pumice
pumice lapilli/ blocks
lithic lapilli/ blocks
accretionary lapilli/ ash pellets
member boundary /entrachron
entrachron
flow-unit boundary
mLT lithofacies type
alluvial sediments
mLT
lmLT
dbLbr
dbLT
mTacc
mLTacc
top not preserved
Flow-unit 4
Flow-unit 2
Flow-unit 1
UTM: 357698/ 3119212
UTM: 357838/ 3119072
UTM: 357946/ 3119035
UTM: 358340/ 3118850
UTM: 358469/ 3118743
A
B
C
D
E
flow-unit
ignimbrite
FU-4
pumice fall
pellet fall ignimbrite
FU-2
pellet fall ignimbrite
FU-1
pumice fall
palaeosol
metres
NW
SE
X'
X
current
present-day exposure
altitude
150
100
0
500
(ash/lapilli/block/boulder)
Poris Formation
300 m
palaeovalley fills
imbrication Member 6
N
2 4 6
n = 40
viewpoint in Fig. 7A
158
119
159

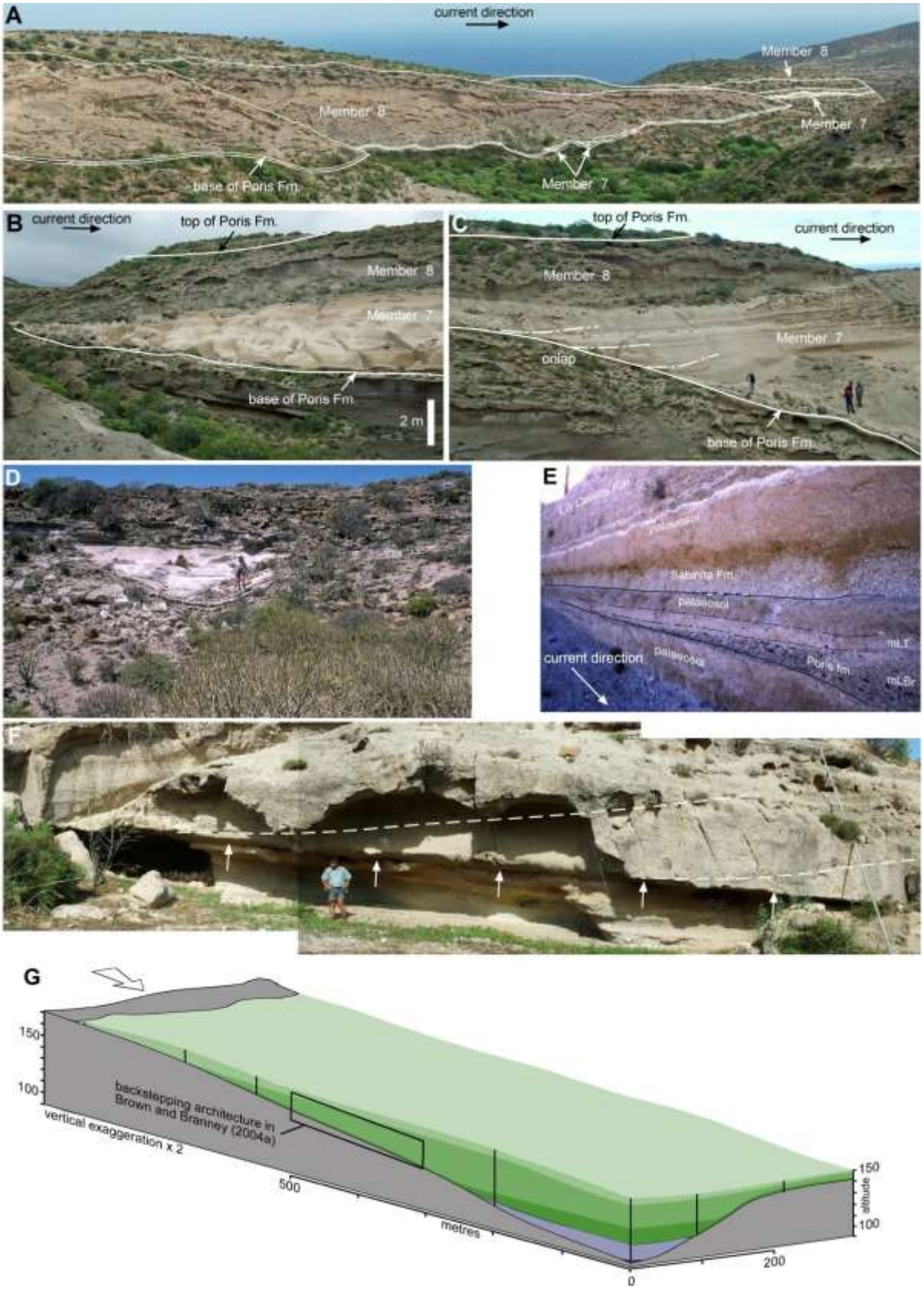
A
current direction
Member 8
Member 8
Member 7
base of Poris Fm.
Member 7
B
current direction
top of Poris Fm.
Member 8
Member 7
base of Poris Fm.
2 m
C
top of Poris Fm.
current direction
Member 8
Member 7
onlap
base of Poris Fm.
D
E
Paleosol
Sabinita Fm.
Paleosol
mLT
current direction
Paleosol
Poris fm.
mLBr
F
G
150
100
backstepping architecture in
Brown and Branney (2004a)
vertical exaggeration x 2
500
metres
0
200
150
100
altitude

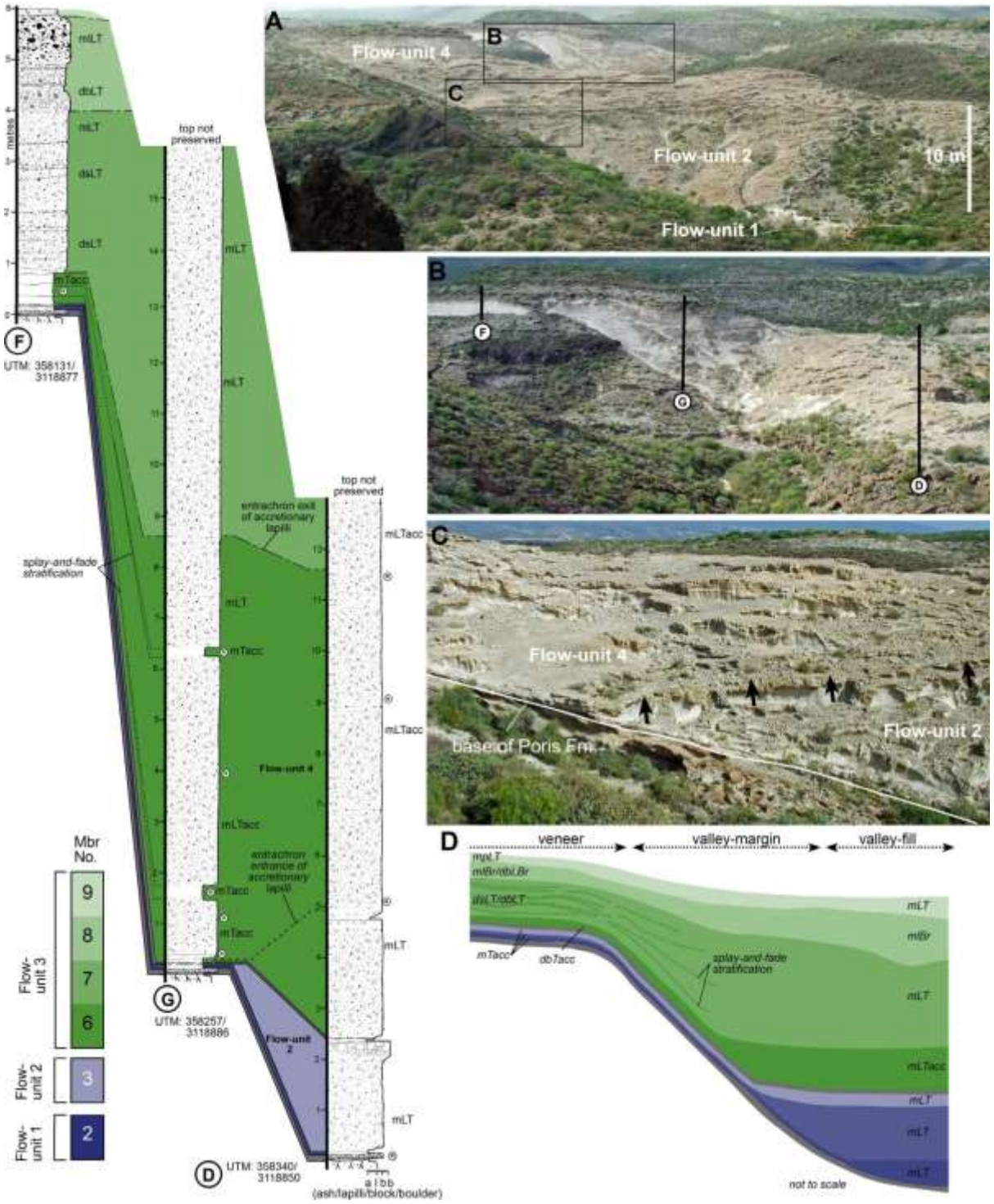
A
Flow-unit 4
B
C
Flow-unit 2
10 m
Flow-unit 1
B
F
G
D
C
Flow-unit 4
base of Poris Fm.
Flow-unit 2
D
veneer
valley-margin
valley-fill
mLT
mBr
mLTacc
not to scale
mLT
dbLT
mLT
dsLT
dsLT
mTacc
F
UTM: 358131/
3118877
top not
preserved
mLT
mLT
splay-and-fade
stratification
mLT
mTacc
Flow-unit 4
mLTacc
mTacc
mTacc
G
UTM: 356257/
3118886
top not
preserved
mLTacc
mLTacc
mLT
Flow-
unit 2
mLT
D
UTM: 358340/
3118850
a | bb
(ash/lapilli/block/boulder)
Mbr
No.
Flow-
unit 3
9
8
7
6
Flow-
unit 2
3
Flow-
unit 1
2


A
current
thin veneer ignimbrite
mantling lee side of cone
ignimbrite in B
B
Fasnia Formation ignimbrite
Plinian fall deposit
and thin ignimbrite
base of formation

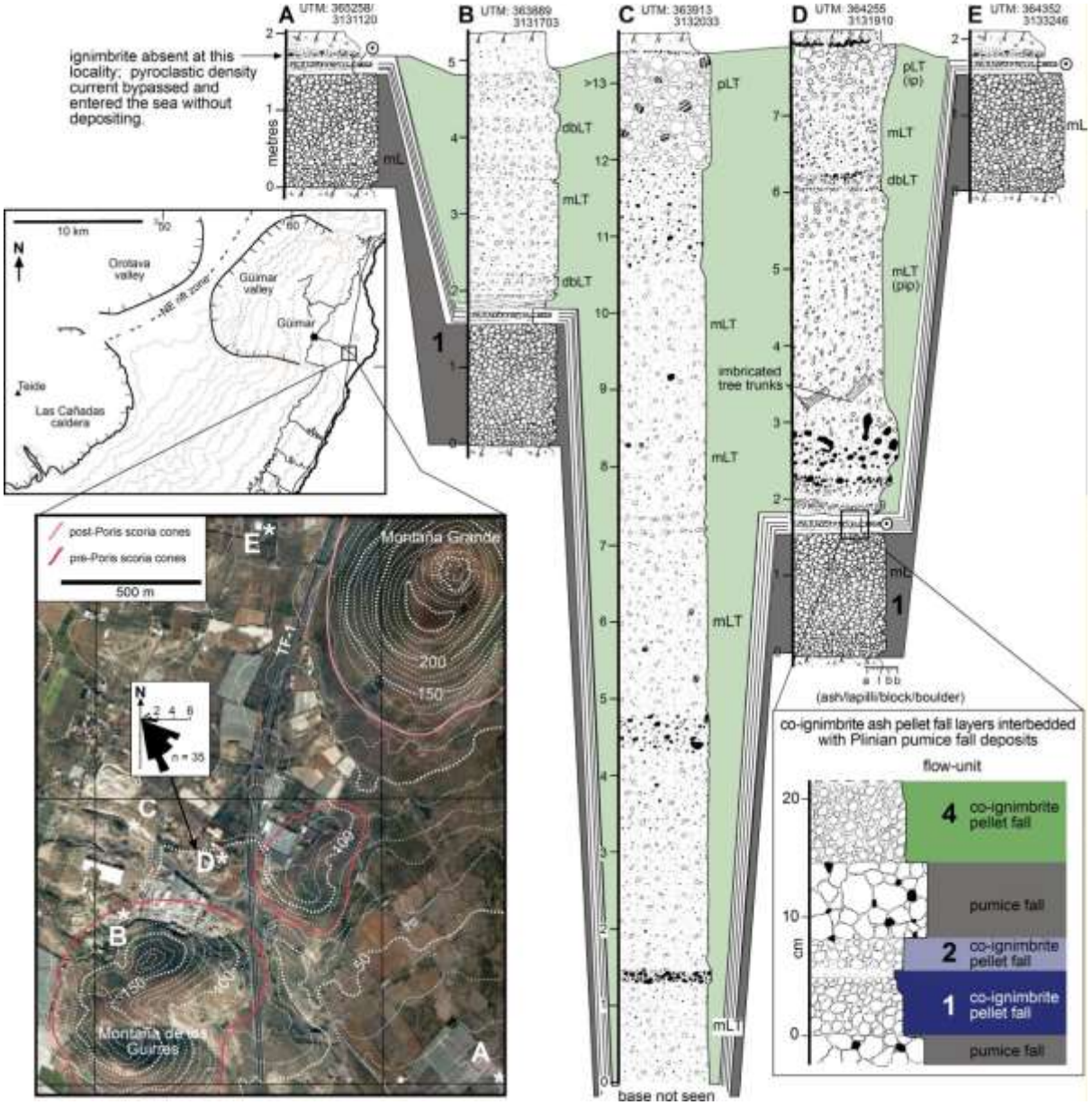
A UTM: 360258/ 3131120
B UTM: 363889 3131703
C UTM: 363913 3132033
D UTM: 364255 3131910
E UTM: 364352 3133246
ignimbrite absent at this locality; pyroclastic density current bypassed and entered the sea without depositing.
metres
mL
dbLT
mLT
pLT
pLT (ip)
mLT (pip)
imbricated tree trunks
base not seen
(ash/lapilli/block/boulder)
10 km
Orotava valley
NE rift zone
Güimar valley
Güimar
Teide
Las Cañadas caldera
post-Poris scoria cones
pre-Poris scoria cones
500 m
Montaña Grande
TF-1
Montaña de las Güimas
n = 35
co-ignimbrite ash pellet fall layers interbedded with Plinian pumice fall deposits
flow-unit
4 co-ignimbrite pellet fall
pumice fall
2 co-ignimbrite pellet fall
1 co-ignimbrite pellet fall
pumice fall
cm

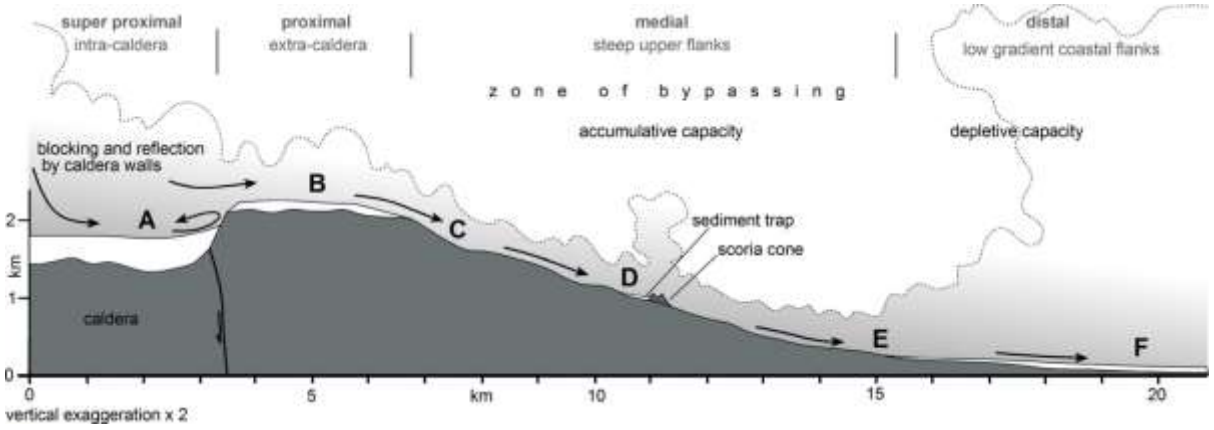
super proximal
intra-caldera
proximal
extra-caldera
medial
steep upper flanks
distal
low gradient coastal flanks
z o n e o f b y p a s s i n g
accumulative capacity
depletive capacity
blocking and reflection
by caldera walls
A
B
C
D
E
F
sediment trap
scoria cone
caldera
km
2
1
0
0
5
km
10
15
20
vertical exaggeration x 2

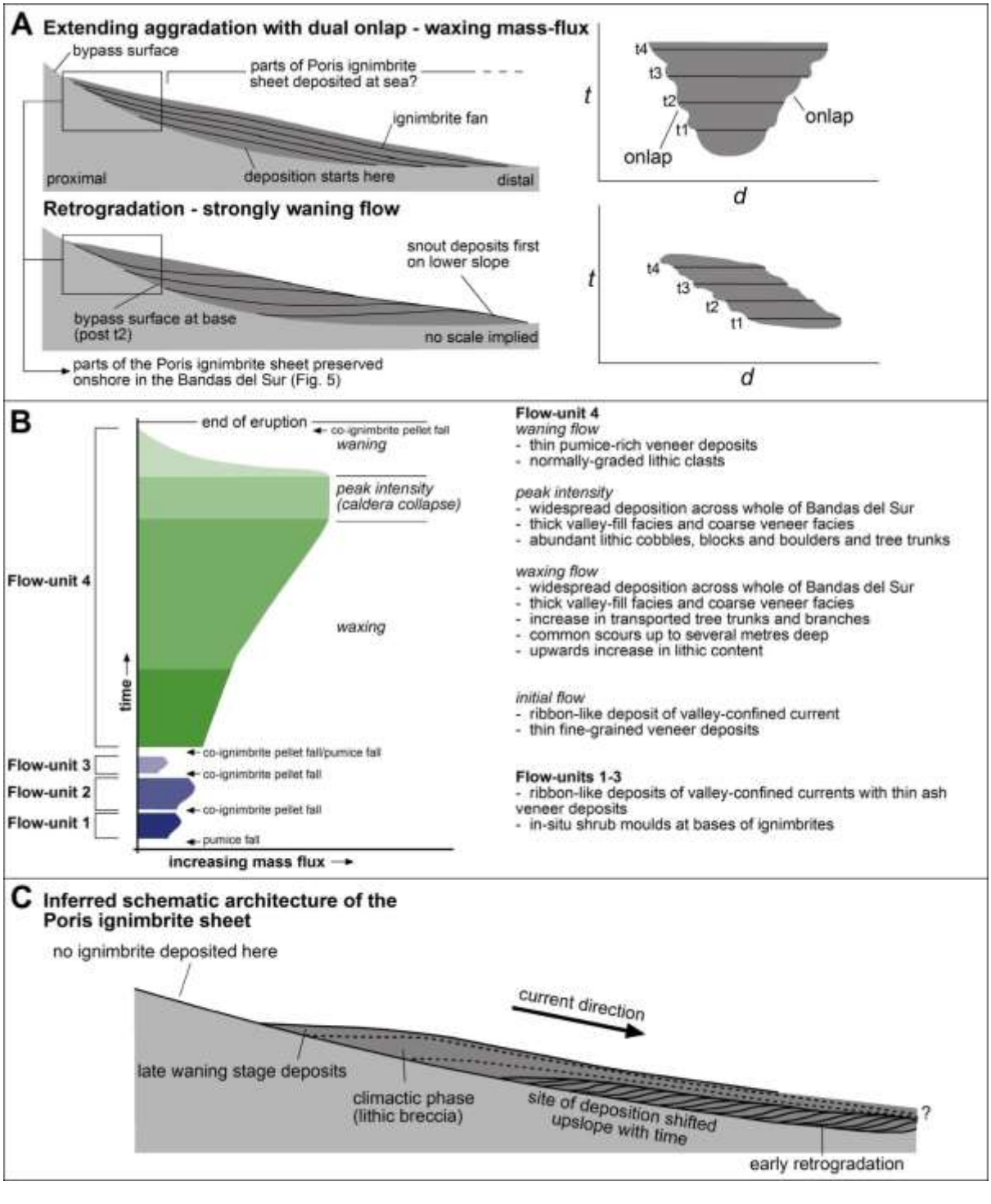
A
Extending aggradation with dual onlap - waxing mass-flux
bypass surface
parts of Poris ignimbrite sheet deposited at sea?
ignimbrite fan
proximal
deposition starts here
distal
t
t4
t3
t2
t1
onlap
onlap
d
Retrogradation - strongly waning flow
snout deposits first on lower slope
bypass surface at base (post t2)
no scale implied
parts of the Poris ignimbrite sheet preserved onshore in the Bandas del Sur (Fig. 5)
t
t4
t3
t2
t1
d
B
end of eruption
co-ignimbrite pellet fall
waning
peak intensity (caldera collapse)
waxing
Flow-unit 4
time
Flow-unit 3
Flow-unit 2
Flow-unit 1
co-ignimbrite pellet fall/pumice fall
co-ignimbrite pellet fall
co-ignimbrite pellet fall
pumice fall
increasing mass flux
Flow-unit 4
waning flow
- thin pumice-rich veneer deposits
- normally-graded lithic clasts
peak intensity
- widespread deposition across whole of Bandas del Sur
- thick valley-fill facies and coarse veneer facies
- abundant lithic cobbles, blocks and boulders and tree trunks
waxing flow
- widespread deposition across whole of Bandas del Sur
- thick valley-fill facies and coarse veneer facies
- increase in transported tree trunks and branches
- common scours up to several metres deep
- upwards increase in lithic content
initial flow
- ribbon-like deposit of valley-confined current
- thin fine-grained veneer deposits
Flow-units 1-3
- ribbon-like deposits of valley-confined currents with thin ash veneer deposits
- in-situ shrub moulds at bases of ignimbrites
C
Inferred schematic architecture of the Poris ignimbrite sheet
no ignimbrite deposited here
current direction
late waning stage deposits
climactic phase (lithic breccia)
site of deposition shifted upslope with time
?
early retrogradation